

Phospholipid Scramblase 1 Is Secreted by a Lipid Raft-dependent Pathway and Interacts with the Extracellular Matrix Protein 1 in the Dermal Epidermal Junction Zone of Human Skin*

Received for publication, April 20, 2010, and in revised form, August 26, 2010. Published, JBC Papers in Press, September 24, 2010, DOI 10.1074/jbc.M110.136408

Joseph Merregaert^{†1,2}, Johanna Van Langen^{†1}, Uwe Hansen[§], Peter Ponsaerts^{¶3}, Abdoelwaheb El Ghalbzouri^{||}, Ellen Steenackers[‡], Xaveer Van Ostade^{**}, and Sandy Serçu^{†4}

From the [†]Laboratory of Molecular Biotechnology and the ^{**}Laboratory of Protein Science, Proteomics, and Epigenetic Signaling, Department of Biomedical Sciences, and the [¶]Laboratory of Experimental Hematology, Vaccine and Infectious Disease Institute, University of Antwerp, 2610 Wilrijk, Belgium, the [§]Department of Physiological Chemistry and Pathobiochemistry, University Hospital of Muenster, Muenster 48149, Germany, and the ^{||}Department of Dermatology, Leiden University Medical Center, Leiden 2333 AL, The Netherlands

We examined the interaction of ECM1 (extracellular matrix protein 1) using yeast two-hybrid screening and identified the type II transmembrane protein, PLSCR1 (phospholipid scramblase 1), as a binding partner. This interaction was then confirmed by *in vitro* and *in vivo* co-immunoprecipitation experiments, and additional pull-down experiments with GST-tagged ECM1a fragments localized this interaction to occur within the tandem repeat region of ECM1a. Furthermore, immunohistochemical staining revealed a partial overlap of ECM1 and PLSCR1 in human skin at the basal epidermal cell layer. Moreover, in human skin equivalents, both proteins are expressed at the basal membrane in a dermal fibroblast-dependent manner. Next, immunogold electron microscopy of ultrathin human skin sections showed that ECM1 and PLSCR1 co-localize in the extracellular matrix, and using antibodies against ECM1 or PLSCR1 cross-linked to magnetic immunobeads, we were able to demonstrate PLSCR1-ECM1 interaction in human skin extracts. Furthermore, whereas ECM1 is secreted by the endoplasmic/Golgi-dependent pathway, PLSCR1 release from HaCaT keratinocytes occurs via a lipid raft-dependent mechanism, and is deposited in the extracellular matrix. In summary, we here demonstrate that PLSCR1 interacts with the tandem repeat region of ECM1a in the dermal epidermal junction zone of human skin and provide for the first time experimental evidence that PLSCR1 is secreted by an unconventional secretion pathway. These data suggest that PLSCR1 is a multifunctional protein that can function both inside and outside of the cell and together with ECM1 may play a regulatory role in human skin.

The human *ECM1* gene (11 exons) is located on chromosome 1q21.2 (1, 2) and encodes four splice variants. ECM1a (without exon 5a) is expressed in basal keratinocytes, dermal blood vessels, and adnexal epithelia, including hair follicles and glands, whereas ECM1b, which lacks exon 7, is expressed in the spinous and granular layers of the epidermis (3–5). ECM1c was found in the basal layer of the epidermis (6), and a fourth splice variant results in a truncated protein of 57 amino acids (7). The ECM1 protein contains a 19-amino acid signal peptide followed by four domains: a cysteine-free N-terminal segment, two tandem repeats, and a C-terminal segment. The two tandem repeats and the C-terminal domain contain cysteines in a typical CC-(X_{7–10})C arrangement that is capable of forming protein double loops that could be involved in protein-protein interactions (1, 8). More recently, a rudimentary three-dimensional model divided the ECM1a protein into four distinct domains: an NH₂-terminal domain forming α -helical structures, followed by three domains, whose amino acid sequences were highly comparable with the third domain of human serum albumin: SASDL2 (serum albumin subdomain-like 2), SASDL3, and SASDL4 (9).

The function of ECM1 has not yet been elucidated in detail; however, it has been reported that ECM1 could act as a novel paracrine factor involved in the regulation of endochondral bone formation (10, 11), is capable of stimulating vascular endothelial cell proliferation and blood vessel formation (12). Moreover, ECM1 is involved in skin differentiation (3) and is a susceptibility locus for ulcerative colitis (13). Its function in skin biology has been highlighted by *ECM1* loss of function mutations that have been recognized as the cause of a rare autosomal recessive genodermatosis, lipoid proteinosis, also known as hyalinosis cutis et mucosae or Urbach-Wiethe disease (OMIM 247100) (14–16). Recent studies identified autoantibodies against the ECM1 protein in lichen sclerosus, also characterized by fragility and hyalinization of the upper dermis (17, 18). In skin, further clues to its physiological role have been suggested by the discovery of interactions with perlecan, fibulin-1C/1D, fibulin-3, and matrix metalloproteinase 9 (6, 9, 18, 20). Perlecan is a major heparan sulfate proteoglycan of the basement membrane, whereas fibulin-1 and fibulin-3 belong to a

* This work was supported in part by the Deutsche Forschungsgemeinschaft (SFB492, TPA2).

[†] Both authors contributed equally to this work.

² To whom correspondence should be addressed: Universiteitsplein 1, 2610 Wilrijk, Belgium. Tel.: 32-3-2652311; Fax: 32-3-8202339; E-mail: joseph.merregaert@ua.ac.be.

³ Recipient of a postdoctoral fellowship of the "Fund for Scientific Research Flanders."

⁴ Recipient of a Ph.D. fellowship from the "Instituut voor de Aanmoediging van Innovatie door Wetenschap en Technologie in Vlaanderen." Present address: EggCentris NV, J. Wybranlaan 40, 1070 Anderlecht, Belgium.

PLSCR1 Interacts with ECM1

family of proteins that are associated with basement membranes and elastic extracellular matrix fibers. Matrix metalloproteinase 9 is a proteolytic enzyme that degrades several extracellular matrix components.

The yeast two-hybrid genetic system has proven to be an efficient tool for examination of protein-protein interactions (21). We have investigated the interaction of ECM1a with other extracellular matrix proteins within the cutaneous basement membrane zone by screening a human foreskin epidermal keratinocyte cDNA library cloned into a vector containing the GAL4 activation domain. We used full-length ECM1a cDNA (hcDNA) and a fragment of ECM1a (SASDL2+; aa⁵ 177–361), containing a full SASDL2 domain and a part of SASDL3, as bait (9). Both screens identified PLSCR1 (phospholipid scramblase 1) as a possible ECM1a binding partner. PLSCR1 is a calcium-binding, palmitoylated, type II endofacial plasma membrane protein with a long cytoplasmic N-terminal domain followed by a single predicted transmembrane helix near the C terminus. Together with three other members identified in humans, it belongs to the phospholipid family of scramblases believed to carry out calcium-dependent, nonspecific, and bidirectional movement (“scrambling”) of phospholipids across the plasma membrane (reviewed in Refs. 22 and 23).

In this study, we demonstrate ECM1a-PLSCR1 interaction, mediated by the ECM1a tandem repeat region, outside the cell in the dermal epidermal junction (DEJ) zone of human skin. Whereas ECM1 is readily secreted via the Golgi system, PLSCR1 displays a more complex cellular distribution. We here describe PLSCR1 to be localized at the cell membrane, in endosomal vesicles, and in the nucleus, thereby excluding intracellular interaction with ECM1. Furthermore, this report provides the first experimental evidence that PLSCR1 is secreted by an unconventional lipid raft-dependent pathway.

EXPERIMENTAL PROCEDURES

Cell Culture—Cultures of normal human keratinocytes were established from human mammary skin surgery, as described earlier (24). Keratinocyte medium used for culturing normal human keratinocytes consisted of Dulbecco's modified Eagle's medium (DMEM) and Ham's F-12 medium (3:1) supplemented with 5% (v/v) HyClone calf serum (Greiner), 1 μ M hydrocortisone, 1 μ M isoproterenol, 0.1 μ M insulin. For experiments, second passages were used. Cultures of human dermal fibroblasts were established as described before (24). They were cultured in DMEM, supplemented with 5% (v/v) FCS (Invitrogen), penicillin (100 IU/ml), and streptomycin (100 μ g/ml) (ICN Biomedicals, Inc). Passages 2–5 were used for the experiments. Cultures of HaCaT cells, a spontaneously immortalized human keratinocyte cell line, were maintained in DMEM (Sigma-Aldrich), supplemented with 10% (v/v) sterile-filtered fetal bovine serum (Sigma-Aldrich), 2% L-glutamine (Invitrogen), 100 μ g/ml streptomycin, and 100 IU/ml penicillin (Invitrogen) at 37 °C in a humidified atmosphere with 5% CO₂. For inhibition of the endoplasmic reticulum/Golgi secretory transport, 25 ng/ml

brefeldin A (Sigma-Aldrich) was added to a HaCaT cell culture for 48 h (25). Palmitoylation was metabolically inhibited by treating HaCaT cultures with 2-bromo-palmitate (Sigma-Aldrich) overnight at 50 μ M (26). To deplete cellular cholesterol, HaCaT cells (1×10^6) were pretreated with methyl- β -cyclodextrin (10 mM) (Sigma-Aldrich) for 1 or 7 h at 37 °C. As an exosome inhibitor, dimethyl amiloride (Sigma-Aldrich) at 15 nM was added to HaCaT cell cultures during 7 h at 37 °C.

For creating HaCaT cell lines stably overexpressing eGFP-PLSCR1 or hemagglutinin (HA)-PLSCR1, cells were transfected at 80% confluence using the Amaxa[®] cell line Nucleofector[®] kit V (Lonza). After 2 weeks of growth in antibiotics-supplemented medium (800 μ g/ml Geneticin (Invitrogen) for HA-PLSCR1-transfected cells and 400 μ g/ml hygromycin (Invitrogen) for eGFP-PLSCR1-transfected cells), positive clonal cell lines were selected after limiting dilution and screening by immunoblotting (for HA-PLSCR1 transfectants), or cells surviving antibiotics selection were pre-enriched for high eGFP expression by cell sorting (FACS AriaII cell sorter, BD Biosciences) and subsequently clonal cell lines with high expression of eGFP-PLSCR1 were selected by flow cytometry (see below). For induction of HaCaT cell differentiation, 1 ng/ml 12-*O*-tetradecanoylphorbol-13-acetate (TPA) was added to the cell cultures as described previously (3).

Reconstruction of Human Skin Equivalents—Hydrated collagen gels were prepared using 4 mg/ml collagen solution isolated from rat tails, as described in detail elsewhere (27). Briefly, the collagen solution was used directly or mixed at 4 °C with fibroblast suspension to reach a final density of 1×10^5 cells/ml. Subsequently, 2.5 ml of collagen mixture was added to a filter insert (6-well plates; Costar). After gel polymerization, culture medium was added, and the collagen matrices were subsequently incubated overnight. For the generation of reconstructed epidermis, keratinocyte cultures were seeded onto fibroblast-free (organotypic keratinocyte monocultures) or fibroblast-populated collagen matrices (organotypic keratinocyte-fibroblast co-cultures). The cultures were incubated overnight in keratinocyte medium containing 5% (v/v) serum, followed by culturing in medium supplemented with 1% serum. Lifting of the collagen matrices at the air/liquid interface was conducted after overnight incubation, and serum-free medium was used 1 day after air exposure. The cultures were grown for 14 days at the air/liquid interface in serum-free medium. In some experiments, the cultures were supplemented with EGF (1 ng/ml) (Sigma-Aldrich). Culture medium was renewed twice a week. After 2 weeks, culture at the air/liquid interface the skin-equivalent cultures were harvested and used for immunohistochemical analysis.

Bacterial and Mammalian Expression Vectors—To determine which part of ECM1a is responsible for binding to PLSCR1, five genetically engineered ECM1a recombinant fragments fused to glutathione *S*-transferase (GST) were used: Δ NH₂ (representing aa 32–340), Δ P_x/COOH (aa 203–432), Δ s/COOH (aa 480–540), Δ s/ex7 (aa 203–390), and Δ Ds/COOH (aa 340–540). These five GST-ECM1a fusion proteins were purified as described before (4). The expression vector of eGFP-PLSCR1 was obtained from Dr. S. Benichou (28). The eukaryotic expression vector containing the

⁵ The abbreviations used are: aa, amino acids; DEJ, dermal epidermal junction; eGFP, enhanced GFP; EGFR, EGF receptor; LN, laminin; TPA, 12-*O*-tetradecanoylphorbol-13-acetate; GAM-PE, phycoerythrin-labeled goat anti-mouse.

TABLE 1
Yeast-two-hybrid primers

Primers	Sequences
Y2hECM1aF	5'-ATGCGACATATGGCCTCTGAGGGAGGCTTCACGGC-3'
Y2hECMaR	5'-CGATGAGGATCCTCATTCTTCCTGGGCTCAGAGGTG-3'
Y2hSASD2NdeIF	5'-GCTAGGCATATGAACCAAATCTGCCTTCCTAACCG-3'
Y2hSASD2BamHIR	5'-CGATGAGGATCCGGCCTTCCATGTACAGGTGTG-3'
Y2hScrF	5'-CGATGATGAAGATACCCAC-3'
Y2hScrR	5'-GTGCACGATGCACAGTTGAAG-3'
PLSCRf	5'-TACCCATACGACGTACCAGATTACGCTCAAATGGACAAACAAAACCTCACAGATGAAT-3'
PLSCRr	5'-CGGGTGAATTCACTGGCCTCCATGGCCAACCACACTCCTGATTTTTGTCTCTG-3'
HA-PLSCR1IRESHygF	5'-GTAGTACCAGTGTGCTGGATGGCTTCTAGCTATCCTTATG-3'
HA-PLSCR1IRESHygR	5'-GTAGTAGCGGCCCTACACACTCCTGATTTTTG-3'

HA-tagged PLSCR1 was made by PCR amplification using pAS1B plasmid as template and the appropriate primers, HA-PLSCR1IRESHygF and HA-PLSCR1IRESHygR (Table 1) (28). The PCR product was subcloned in the BstXI-NotI sites of the pIRESHyg1 vector (Clontech).

Yeast Two-hybrid Constructs—hECM1a and a shorter form, SASDL2+ (aa 177–361), were amplified by PCR, with primers Y2hECM1aF and Y2hECM1aR and primers Y2hSASD2NdeIF and Y2hSASD2BamHIR, respectively (Table 1), using a previous construct (BU52) containing the full-length ECM1a sequence as template. Both fragments were inserted into the pGBKT7 vector (Clontech) between NdeI and BamHI sites in frame with the GAL4 activation domain and the Myc tag. The minimal sequence of PLSCR1 (aa 1–318) was amplified by PCR, with the PLSCRf and PLSCRr primers (Table 1), using their primordial sequence in the PGAD10 vector (Clontech) as template. The PLSCR1 fragment was inserted in the NdeI site in frame with the hemagglutinin tag into the pGADT7-vector (Clontech), which has a T7 promoter, necessary for *in vitro* transcription/translation.

Yeast Two-hybrid Library Screening—The Matchmaker two-hybrid system (Clontech) was used to screen a foreskin library constructed in the pGAD10 vector (Clontech). Competent AH109 yeast cells, which contain four reporter genes (*ADE2*, *HIS3*, *lacZ*, and *MEL1*), were prepared and transformed with the pGBKT7 constructs, following the YeastmakerTM Transformation System 2 instructions (Clontech). After 4 days of growth at 30 °C, colonies were used for a second transformation with the human foreskin keratinocyte library. The reactions were streaked onto quadruple dropout plates lacking adenine, histidine, leucine, and tryptophan. Protein interactions were analyzed 10 days later and confirmed by a simple blue/white colony screening. Through interaction of both proteins, the GAL4 DNA-binding domain and DNA activation domain are reunited, thus forming a transcriptionally active GAL4 transcription factor, which will result in α -galactosidase transcription (blue colonies). The plasmids from the blue colonies were extracted using the Zymoprep yeast plasmid miniprep kit (Baseclear). Two microliters of yeast DNA was transformed into DH5 α *Escherichia coli*. To screen for single transformants, the DH5 α cells were plated onto LB agar plates containing 100 μ g/ml ampicillin. Colonies that grew on these plates were transferred into 5 ml of LB and cultured overnight at 37 °C. Using the Genelute plasmid miniprep isolation kit (Sigma), the activation domain vectors were isolated for sequencing.

DNA Sequencing and Inset Identification—Using the sequencing primers Y2hScrF and Y2hScrR (Table 1) for the

pGAD10 vector, the inserts of the yeast plasmids were sequenced. The AB 3730 DNA analyzer in combination with the very sensitive ABI PRISM[®] BigDyeTM terminator cycle sequencing kits (Applied Biosystems) were used to yield long runs with low background. We searched the BLAST data base on the NCBI Web site to identify the inserts of the human foreskin cDNA library that interacted with ECM1a fragments. The PLSCR1 insert was confirmed to be cloned in frame in the pGAD10 vector.

In Vitro Transcription/Translation and Co-immunoprecipitation—In order to generate peptides of the ECM1a fragments and PLSCR1 clones, *in vitro* transcription/translation of 1 μ g of pGADT7 and PGBKT7 constructs was performed in the presence of 2 μ l of [³⁵S]methionine (GE Healthcare) and 40 μ l of TNTTM reticulocyte lysate (Promega Corp.). The 50- μ l reactions were incubated for 90 min at 30 °C and used for *in vitro* co-immunoprecipitation. The *in vitro* transcribed proteins were used for *in vitro* co-immunoprecipitation with the BD Bioscience Matchmaker Co-IP kit (Clontech). An amount of 10 μ l of both ECM1a fragments was individually mixed with 10 μ l of PLSCR1 protein and incubated for 1 h at room temperature. About 10 μ l of the anti-hemagglutinin antibody (Clontech) (the pGADT7 vector carries the hemagglutinin tag sequence) or the anti-c-Myc antibody (Clontech) (the pGBKT7 vector carries the c-Myc tag sequence) was added. After a 1-h incubation at room temperature, the immune complexes were captured with 3 μ l of protein A beads (Clontech). The tubes were centrifuged in a microcentrifuge at 5000 \times g for 10 s. The supernatant was discarded, and the beads were washed five times with 500 μ l of wash buffer 1 and then twice with 600 μ l of wash buffer 2. Then 20 μ l of SDS-PAGE loading buffer (2% SDS and 50 mM Tris-HCl in distilled water, pH 6.8) was added to each reaction tube, and the proteins were denatured by boiling for 5 min. The tubes were then placed on ice and briefly centrifuged at 7000 \times g, and 15 μ l of each supernatant was analyzed by electrophoresis and exposure to Eastman Kodak Co. Biomax XAR films.

In Vivo Co-immunoprecipitation and Immunoblotting—Co-immunoprecipitation experiments were performed on cell lysates or supernatant of the human keratinocyte HaCaT cell line or fibroblast/keratinocyte organotypic co-cultures. Cell lysates from HaCaT cells were obtained at about 80% confluence by incubation with a Nonidet P-40 lysis buffer (10 mM Tris-HCl (pH 7), 200 mM NaCl, 5 mM EDTA, 10% glycerol, 1% Nonidet P-40) in the presence of a protease inhibitor mixture (Roche Applied Science) after rinsing the cells with PBS. Supernatant of the cells was collected after a 24-h incubation with a minimal volume of serum-free medium, followed by centrifu-

PLSCR1 Interacts with ECM1

gation to remove cells and cell debris. Co-immunoprecipitations were performed with 250 μg of protein from cell lysate or supernatant. The samples were precleared by preincubation with protein A-Sepharose 4B beads (15 min, 4 °C; Invitrogen). Beads were pelleted by centrifugation, and supernatant was transferred and incubated with an affinity-purified rabbit polyclonal antibody against ECM1 (EDF, Human Genome Sciences Inc.) or with mouse monoclonal PLSCR1 antibody (Abcam, Cambridge, MA). After 2 h at room temperature, protein A-Sepharose 4B beads were added, and the mixture was incubated overnight at 4 °C. The protein A-Sepharose beads were purified following the protocol of the manufacturer and prepared for SDS-PAGE by adding loading buffer.

The protein samples were denatured by boiling for 5 min, separated on a 10% polyacrylamide gel, and electrophoretically transferred to nitrocellulose membranes (Amersham Biosciences) by blotting for 20 min at 20 V after a 20-min incubation period in transfer buffer. Membranes were blocked with 5% (w/v) milk powder dissolved in PBS with 1% (v/v) Tween for 1 h at 37 °C, followed by an overnight incubation at 4 °C with the primary antibodies dissolved in PBS-Tween containing 5% (w/v) milk powder. Rabbit anti-ECM1 polyclonal antibodies (EDF, Human Genome Sciences), rabbit polyclonal anti-PLSCR1 C terminus antibody (Abcam, Cambridge, MA), and goat anti-GST antibodies (GE Healthcare) were used at a 1:100, 1:500, and 1:1000 dilution, respectively, followed by an incubation with goat anti-rabbit IgG-horseradish-conjugated secondary antibody (Dako) or rabbit anti-goat (Dako) at a 1:2000 or 1:80,000 dilution, respectively, for 1 h at 37 °C. Immunoblots were stained with ECL (GE Healthcare) and developed on BioMax XAR films (PerkinElmer Life Sciences).

To identify the interaction domain of ECM1a involved in PLSCR1 binding, genetically engineered GST-ECM1a recombinant fragments were used (see above) (4). Pull-downs were performed by incubating 40 μg of recombinant GST protein with 100 μl of 50% glutathione-Sepharose 4B beads (Amersham Biosciences) for 24 h at 4 °C, after which 250 μg of HaCaT cell lysate was added and incubated for another 2 h at 4 °C. After centrifugation, the pellet was washed three times with lysis buffer (50 mM Tris-HCl, pH 7.4, 1% Nonidet P-40, 150 mM NaCl, 1 mM EDTA, and proteinase inhibitor), and the protein was eluted from the beads with 1 \times GST elution buffer (10 mM reduced glutathione, 50 mM Tris-HCl, pH 8.0). Gel electrophoresis and Western blotting were performed as described above using goat anti-GST polyclonal antibodies (GE Healthcare) and rabbit polyclonal anti-PLSCR1 C terminus antibodies (Abcam).

Immunohistochemistry—Using snap-frozen sections from native skin and 2-week-old cultured skin equivalents, double immunolabeling was performed with the following antibodies: ECM1 (OAP 12516, Human Genome Sciences), PLSCR1 (AO1) (Abnova), and laminin (LN) 332 (BM165) (a gift from Dr. Aumailley (Cologne, Germany)). For this purpose, tissues were fixed in acetone for 10 min and preincubated for 30 min with 5% normal horse serum. For ECM1 and laminin 332, tissues were incubated for 1 h with polyclonal rabbit anti-ECM1 and monoclonal mouse anti-LN 332 followed by incubation for 1 h with goat anti-mouse Cy3 (1:500) and goat anti-rabbit-FITC (1:200)

(Serotec, Oxford, UK). For the PLSCR1 and LN 332 staining, the samples were first incubated for 1 h with monoclonal mouse anti-LN 332 followed by goat anti-mouse Cy3 (1:500) and then incubated (1 h) with polyclonal mouse anti-PLSCR1, followed by incubation for 1 h with goat anti-mouse FITC (1:200). For the double immunolabeling with ECM1 and PLSCR1, sections were incubated for 1 h with polyclonal rabbit anti-ECM1 and polyclonal mouse anti-PLSCR1, followed by incubation (1 h) with goat anti-mouse Cy3 (1:500) and goat anti-rabbit-FITC (1:200). The OAP 12516 and AO1 antibodies were used in a 1:150 dilution, whereas BM165 was used in a 1:175 dilution. Nuclear staining was performed with 4',6-diamidino-2-phenylindole (DAPI) (1:1000) (Molecular Probes) for 2 min. Finally, tissue samples were mounted with Vectashield (Brunschwig Chemie, Amsterdam, The Netherlands).

HaCaT cells were grown for 24 h on coverslips and fixed with 4% paraformaldehyde for 20 min, followed by immunostaining as described for the frozen skin sections. An affinity-purified rabbit polyclonal anti-ECM1 antibody (EDF antibody, 1:100), a mouse monoclonal antibody to LAMP1, a lysosome marker (H4A3, Abcam), a mouse monoclonal antibody to EEA1, an early endosome marker (1G11, Abcam), and a mouse monoclonal antibody to the 58-kDa Golgi protein (FTCD, Abcam) were used. The signals were visualized using an LSM 510 confocal laser scanner (Zeiss).

Immunogold Electron Microscopy—Freshly obtained human skin was sliced in small pieces and fixed in 4% paraformaldehyde and 0.25% glutaraldehyde in 100 mM sodium cacodylate buffer, pH 7.4, at 4 °C. The samples were rinsed in PBS, dehydrated in an ascending series of ethanol from 30 to 70%, and embedded in the acrylic resin LR White (London Resin Company, UK). Ultrathin sections were cut with an ultramicrotome and collected on Formvar-carbon-coated nickel grids for immunogold electron microscopy. For double labeling, the sections were incubated with 100 mM glycine in PBS for 2 min, washed twice with PBS, and incubated with 2% BSA in PBS for 30 min. Thereafter, polyclonal antibodies against ECM1 (EDF, Human Genome Sciences) diluted 1:50 in 0.2% BSA and mouse monoclonal antibodies against PLSCR1 (Abcam) diluted 1:50 in 0.2% BSA were incubated for 2 h. After washing with PBS, the sections were incubated with gold-conjugated antibodies against rabbit immunoglobulins (18-nm gold particles) and mouse immunoglobulins (12-nm gold particles). Finally, all sections were rinsed with water and stained with uranyl acetate for 8 min. As control experiments, the first antibodies were omitted. Electron micrographs were taken at 80 kV with an EM-410 electron microscope (Philips).

Flow Cytometry—Antibody staining and flow cytometric analysis for detection of PLSCR1 expression were performed both on viable and on fixed/permeabilized HaCaT, HaCaT/eGFP-PLSCR1, and HaCaT/HA-PLSCR1 cell lines. Antibody staining on viable cells will determine the presence of PLSCR1 at the extracellular side of the cell membrane. For this, HaCaT, HaCaT/eGFP-PLSCR1, and HaCaT/HA-PLSCR1 cells were harvested and washed twice with PBS. Next, cells ($1 \times 10^6/100 \mu\text{l}$ /staining) were either non-stained (control), stained with 1 $\mu\text{g}/100 \mu\text{l}$ phycoerythrin-labeled

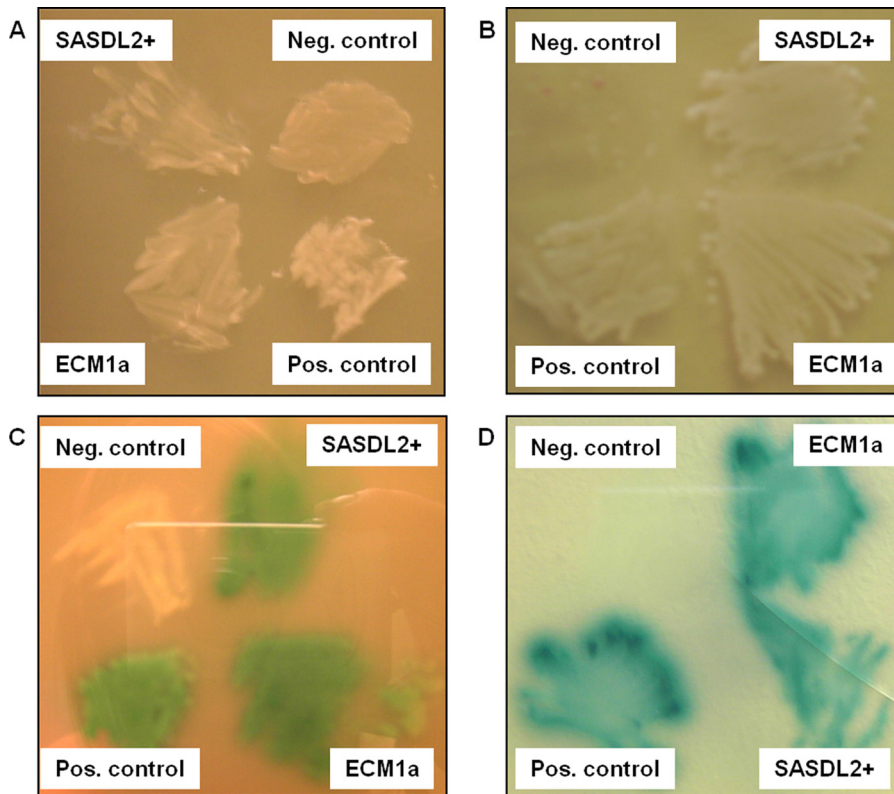


FIGURE 1. Specific interaction between PLSCR1 and ECM1a fragments. The pGBKT7-full-length ECM1a (containing full-length hcDNA of ECM1a) or the PGBKT7-SASDL2+ constructs (containing the serum albumin subdomain-like 2 cDNA+) (aa 177–361) was used as a partner for interaction with the pGADT7-PLSCR1 construct. *A*, all clones were able to grow on plates with triple dropout medium. *B*, the same transfectants were plated on plates with quadruple dropout medium to check for putative interactions. Growth was observed with the positive control (*Pos. control*) (pGBKT7-53/pGADT7-T) as well as with the pGBKT7-ECM1a/pGADT7-PLSCR1 (ECM1a) and pGBKT7-SASDL2+/pGADT7-PLSCR1 (SASDL2+) transfectants. No growth was detected for the negative control (*Neg. control*) (pGBKT7/pGADT7-PLSCR1). *C*, β -galactosidase assays were performed on plates with triple dropout medium. Growth of all of the transfectants was detected. Only the negative control revealed no blue color. *D*, β -galactosidase assays were performed on plates with quadruple dropout medium. No growth and blue coloring were found for the negative control.

goat anti-mouse (GAM-PE; Jackson ImmunoResearch) secondary antibody (control) or 1 μ g/100 μ l mouse anti-PLSCR1 (Abcam), followed by staining with 1 μ g/100 μ l GAM-PE (specific staining), according to previously optimized procedures (29). Following staining, cells were washed once with PBS and analyzed by the Epics-MCL analytical flow cytometer (Beckman Coulter). At least 10,000 cells were analyzed per sample, and flow cytometry results were analyzed with FlowJo software. Antibody staining on fixed/permeabilized cells will determine the presence of PLSCR1, both intracellular and at the extracellular side of the cell membrane (total protein). For this, HaCaT, HaCaT/eGFP-PLSCR1, and HaCaT/HA-PLSCR1 cells were harvested and washed twice with PBS. Next, cells were fixed for 15 min at 4 °C in PBS containing 2% paraformaldehyde. After washing the fixed cell population with PBS, cells were permeabilized for 30 min in ice-cold 70% ethanol at –20 °C. Next, after washing the cell population with PBS, staining for PLSCR1 and flow cytometric analysis was performed as described above.

Pull-down Experiments Using Supraparamagnetic Immunobeads—Extracts from human skin containing suprastructural fragments were obtained by mechanical disruption of tissue and subsequently used for the isolation by supraparamagnetic

immunobeads (Invitrogen) as described before (30, 31). In brief, the supraparamagnetic polystyrene beads covered with affinity-purified secondary antibodies (e.g. sheep anti-rabbit immunoglobulins) were covalently coupled to primary antibodies against ECM1 or PLSCR1 as targets. For that, the beads were incubated with the primary antibodies under continuous rotation overnight at 4 °C. For cross-linking, the coated beads were first resuspended in 0.2 M triethanolamine (pH 8.2) and then incubated for 30 min in 20 mM dimethyl pimelimidate dihydrochloride (Pierce) at room temperature. After magnetic separation, the reaction was stopped by resuspending the bead pellet in 50 mM Tris, pH 7.5, for 15 min. Finally, the beads were washed with PBS and resuspended in PBS containing 0.1% serum albumin. For better purity, the separation step was repeated four times. Magnetic separation was achieved by placing the tubes for 10 min on a permanent magnet (Invitrogen). The bead pellets of each separation step were washed several times with PBS and resuspended in SDS-PAGE loading buffer containing 5% (v/v) β -mercaptoethanol. The resuspended pellets were pooled and analyzed by

immunoblotting and immunogold electron microscopy.

RESULTS

ECM1a Is Capable of Binding to Phospholipid Scramblase 1—A yeast two-hybrid genetic screen was used to identify putative binding partners of ECM1a and SASDL2+ (aa 177–361), containing the complete SASDL2 and a part of SASDL3 comparable with a part of the tandem repeat region of ECM1a (9). Screening of a human foreskin library, followed by selection on Ade-, Leu-, His-, and Trp-plates, resulted in the isolation of six PLSCR1 sequences, with an overlapping region of 318 aa. The interactions between both full-length ECM1a/SASDL2+ fragment and the minimal PLSCR1 fragment (aa 1–318) were retested using the pGADT7-PLSCR1 and pGBKT7-ECM1a constructs in a one-to-one interaction. The clones resulting from the former transfection were first replated on plates without leucine, tryptophan, and uracyl (triple dropout) to confirm whether the transfection worked properly (Fig. 1A), and the same yeast colonies were replated on minimal quadruple dropout medium to look for false negatives (Fig. 1B). Triple and quadruple dropout medium plates, containing X-gal, were used for further confirmation. The growth of the blue colonies and

PLSCR1 Interacts with ECM1

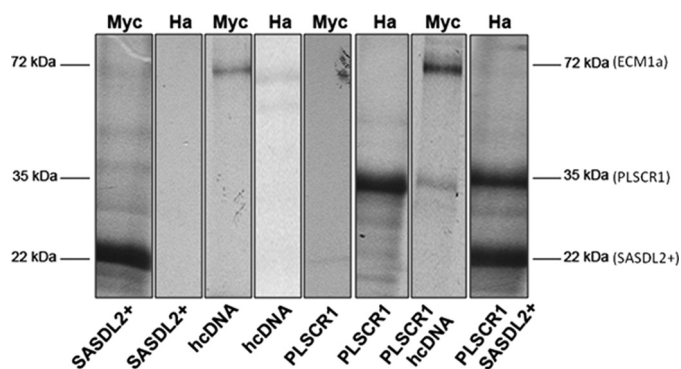


FIGURE 2. *In vitro* co-immunoprecipitation experiments. After *in vitro* transcription/translation with the TNTTM reticulocyte lysate of full-length ECM1a (hcDNA), serum albumin subdomain-like+ (SASDL2+), and phospholipid scramblase 1 (PLSCR1), *in vitro* co-immunoprecipitation was performed with the BD Bioscience Matchmaker Co-IP kit. Both ECM1a fragments tagged with Myc were mixed individually with the HA-tagged PLSCR1 protein and incubated with protein A-beads coated either with anti-hemagglutinin antibody (Ha) or anti-c-Myc antibody (Myc). After SDS-PAGE, the immunoblots were incubated with the Myc or the Ha antibody (indicated at the top).

the intensity of the blue color were comparable with the positive control (Fig. 1, C and D).

Interaction of ECM1a and Phospholipid Scramblase 1 in Cell-free Systems—To corroborate the results obtained with the yeast two-hybrid system, we performed co-immunoprecipitation experiments. The minimal PLSCR1 sequence was cloned into the pGADT7 vector that contains an HA tag. Both ECM1a fragments (hcDNA and SASDL2+) were inserted into the pGBKT7 vector with a c-Myc epitope. The clones were subjected to coupled transcription/translation *in vitro*, after which the proteins were precipitated with antibodies recognizing either the HA epitope or the c-Myc epitope. These results confirm that PLSCR1 interacts with both full-length ECM1a protein and the SASDL2+ ECM1a fragment (Fig. 2, lanes 7 and 8).

PLSCR1 Interacts with the Tandem Repeat Region of ECM1a—The specificity of the interaction between ECM1a and PLSCR1 was also confirmed by a co-immunoprecipitation assay performed on cell lysates of HaCaT cells. Precipitates were then analyzed by immunoblotting with anti-ECM1 antibodies (EDF) and anti-PLSCR1 C terminus antibodies (Fig. 3B). Endogenous PLSCR1 and ECM1 were detected as 35- and 65-kDa proteins in cell lysates immunoprecipitated with anti-ECM1 and anti-PLSCR1 C terminus antibody, respectively, and not in lysates treated with the control isotype antibody. In order to map the ECM1a region required for PLSCR1 binding, GST pull-down experiments were performed using five overlapping GST-ECM1a recombinant fusion fragments (Δ NH₂, Δ Px/COOH, Δ S/COOH, Δ S/ex7, and Δ Ds/COOH) covering the entire ECM1a protein sequence (Fig. 3C). The GST-fused fragments of ECM1a were immobilized on GST-Sepharose beads before incubation with a lysate of HaCaT cells. The fragment length of the GST-ECM1a recombinant fusion proteins was confirmed on an anti-GST immunoblot (Fig. 3D). The resulting GST pull-downs confirmed the interaction of PLSCR1 with the Δ NH₂, Δ Px/COOH, and Δ S/ex7 fragments (Fig. 3E). Identical results were also obtained with lysates from fibroblast/keratinocyte organotypic co-cultures, representing functional skin equivalents (data not shown). Together, these results demon-

strate the binding between PLSCR1 and three fragments covering the tandem repeat region of ECM1a consisting largely of exon 7 and as such indicate that PLSCR1 is a novel specific ligand for the aa 203–349 region of ECM1a.

Partial Expression Overlaps between ECM1 and PLSCR1 in Human Skin—Due to the lack of information about the PLSCR1 expression in human skin, we chose to investigate the potential expression overlap of this protein with ECM1 in this organ. After co-treatment of frozen sections of human skin with a rabbit polyclonal anti-ECM1 antiserum (Protein Tech Group Inc.) and a mouse polyclonal anti-PLSCR1 (Abnova) antibody, we found that ECM1 was expressed at the basal layer of the epidermis (Fig. 4A (I)) and overlapped with LN 332 at the basement membrane (arrow), whereas PLSCR1 was expressed throughout the epidermis as a clearly visible intracellular staining (Fig. 4A (II)). Also, this protein showed overlaps with LN 332 (arrow). The anti-ECM1 serum (Protein Tech Group Inc.) recognizes mainly the ECM1a isoform of ECM1. Co-localizations of ECM1, PLSCR1, and LN 332 are shown in Fig. 4A.

ECM1 and PLSCR1 Are Localized at the Basal Membrane in Reconstructed Human Skin Equivalents; Expression Is Regulated by Dermal Fibroblasts and EGF—Organotypic keratinocyte mono- and co-cultures were analyzed for the expression of ECM1 using the ECM1 antibody OAP 12516. The anti-PLSCR1 antibody was used to detect PLSCR1 expression. As shown in Fig. 4B (II), stratified epidermis was formed even in the absence of fibroblasts, but the viable compartment consisted only of about four cell layers. The effects of EGF on ECM1 and PLSCR1 expression in organotypic keratinocyte monocultures were investigated as well. This cytokine is an excellent control to follow basement membrane formation because it activates the expression of various basement membrane proteins (32). For this purpose, 1 ng/ml EGF was supplemented to the culture medium of skin cultures, cultured for 2 weeks at the air/liquid interface. Double immunolabeling revealed the deposition of ECM1 and PLSCR1 proteins in the basal cell layers of organotypic keratinocyte cocultures (Fig. 4B (I)) and in organotypic keratinocyte monocultures supplemented with EGF (Fig. 4B (III)). In addition, both proteins revealed a co-localization with LN 332. In organotypic keratinocyte monocultures (Fig. 4B (II)) without growth factor supplementation, no expression of ECM1, PLSCR1, and LN 332 could be detected. Together, these findings indicate that only in the presence of fibroblasts or following the addition of EGF, ECM1 as well as PLSCR1 are synthesized and deposited at the DEJ zone of reconstructed skin.

PLSCR1 Co-localizes with ECM1 in the DEJ Zone of Human Skin—In order to obtain a more detailed notion of the site of interaction between ECM1 and PLSCR1 in the DEJ zone, immunogold electron microscopy was performed on ultrathin sections of human skin. Fig. 5 (A–D) shows that both ECM1 and PLSCR1 can be found in the extracellular matrix of the DEJ zone. Both proteins were co-localized within network-like suprastructures within the dermal basement membrane as well as close to dermal collagen fibrils. Moreover, the proteins are also found in the basal keratinocytes, but here, co-localization is not so evident. The co-localization within the extracellular matrix suggests a physiological role for the ECM1-PLSCR1 interaction in human skin, and, above all, these results are the

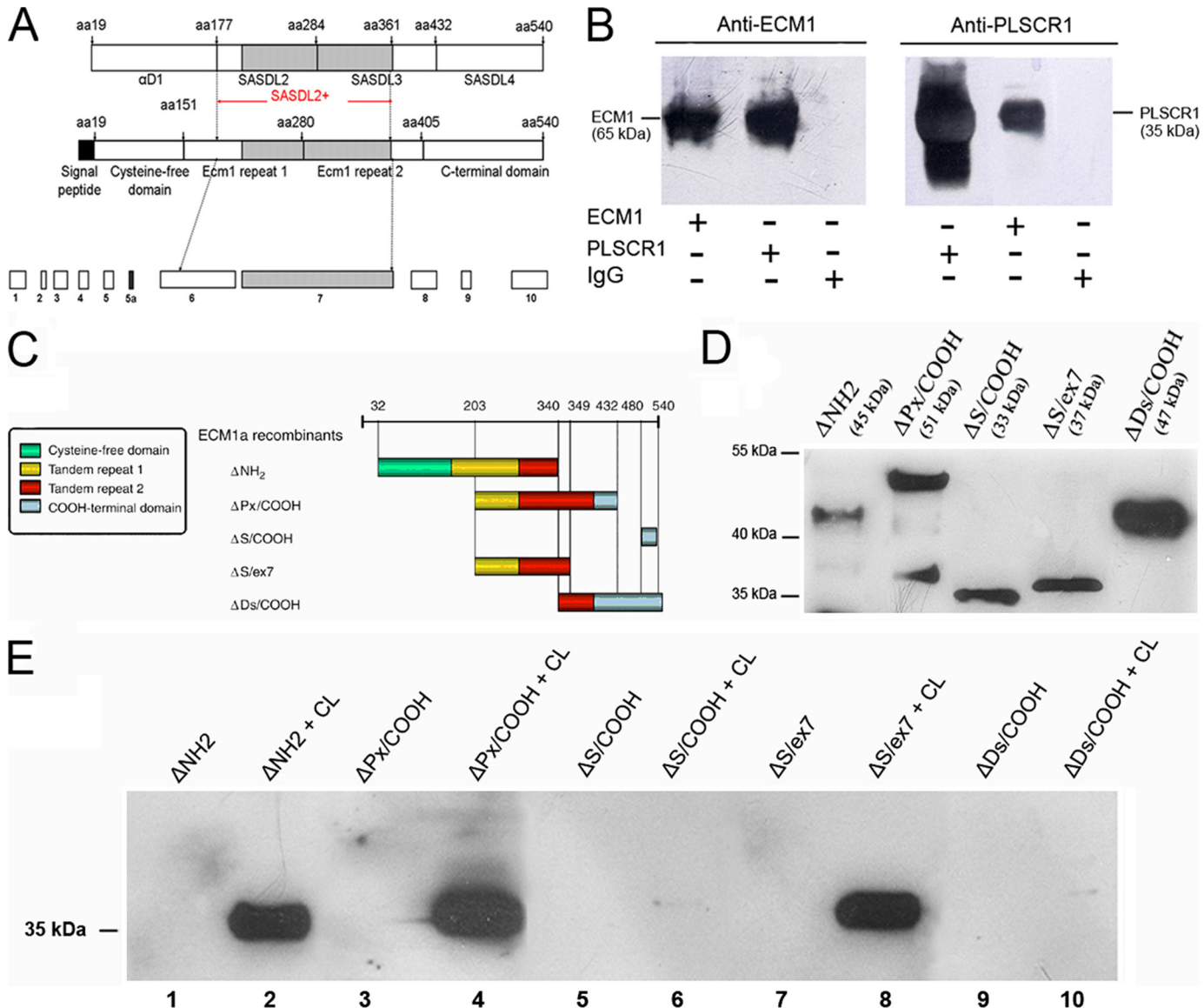


FIGURE 3. PLSCR1 binds selectively to the tandem repeat region of ECM1a *in vivo*. *A*, schematic overview of the exon (*bottom*) and protein structure of ECM1a with its domains. *B*, HaCaT cell lysates (CL) were co-immunoprecipitated with EDF anti-ECM1, a polyclonal anti-PLSCR1 antibody, or an irrelevant IgG as a negative control. Immunoblotting with the complementary antibodies (indicated at the *top*) showed interaction in both directions. *C*, schematic illustration of the ECM1a fragments and the covered domains that were fused with a GST tag. *D*, purified GST-fused ECM1a fragments were checked for the correct lengths. *E*, the fragments were incubated with cell lysates of human HaCaT cells, and GST pull-downs were followed by immunoblotting with the anti-PLSCR1 C terminus antibody. Controls with only purified fragment were all negative (*lanes 1, 3, 5, 7, and 9*). The pull-down results show that PLSCR1 (35 kDa) is able to associate with the ΔNH₂, ΔPx/COOH, and ΔS/ex7 fragments (*lane 2, 4, and 8, respectively*) but could not be picked up by the ΔS/COOH and ΔDs/COOH fragments (*lane 6 and 10, respectively*). These three fragments align with the tandem repeat region of ECM1a (*A*).

first to demonstrate that PLSCR1 can be secreted despite the lack of a secretion signal.

Pull-down Experiments with Human Skin Extracts Using Magnetic Immunobeads—In order to support the ultrastructural results showing a co-localization of PLSCR1 and ECM1 in the extracellular matrix of human skin, pull-down experiments with human skin extracts were performed (Fig. 6). By using antibodies against ECM1 for the isolation of skin suprastructures, PLSCR1 was detected in the obtained bead pellet by immunoblotting. Moreover, by using antibodies against PLSCR1 for the isolation, ECM1 was detected as a component of the isolated suprastructures. Therefore, the pull-down experiments suggest that both ECM1 and PLSCR1 are part of the same suprastructure within the extracellular matrix, which

could be isolated by the use of supraparamagnetic immunobeads. Additionally, ECM1 and PLSCR1 bead pellets were also analyzed by immunogold electron microscopy, revealing that extracellular matrix suprastructures were isolated either by the use of antibodies against ECM1 (Fig. 6*B*) or antibodies against PLSCR1 (Fig. 6*C*).

PLSCR1 Does Not Interact with ECM1 in the Intracellular Compartment—Because of the absence of a secretory signal on PLSCR1, we examined the intracellular localization of PLSCR1 and ECM1 by double immunostaining on HaCaT keratinocytes. Confocal microscopy in Fig. 7*A* shows the presence of ECM1 in secretory vesicles, as expected, whereas PLSCR1 was clearly detectable at the membrane (Fig. 7, *B* and *C*). We therefore conclude that the interaction between ECM1 and PLSCR1

PLSCR1 Interacts with ECM1

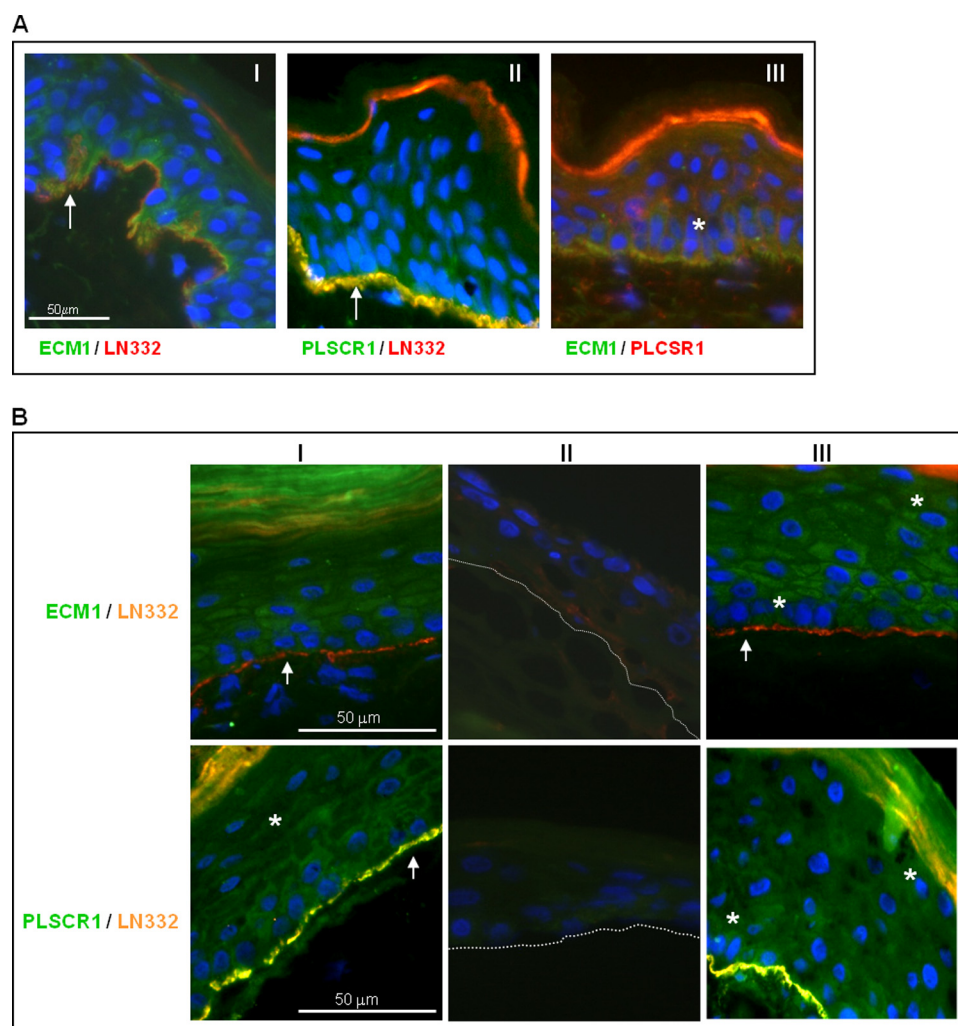


FIGURE 4. Co-localization of ECM1 and/or PLSCR1 with LN 332 in native skin (A) and reconstructed human skin equivalents (B). A, co-localization (orange) at the basement membrane (arrow) of ECM1 (green) with LN 332 (red) (I) and PLSCR1 (green) with LN332 (red) (II). ECM1 (green) is expressed in the basal layers of the human skin, whereas PLSCR1 (red) is expressed through the epidermis (III) (see asterisk for co-localization (orange)). B, fibroblasts and EGF affect ECM1 and PLSCR1 expression in the epidermis. Two-week old air-exposed keratinocyte-fibroblast co-cultures (I) show a clear expression of ECM1 (green) in the basal layers and the deposition of LN 332 (yellow) at the basement membrane (arrow). PLSCR1 (green) also shows expression in the basal layers which shifts toward the upper layers (see asterisk). Organotypic keratinocyte monocultures (II) do not express ECM1, PLSCR1, and LN 332, whereas organotypic keratinocyte monocultures supplemented with 1 ng EGF (III) show an up-regulation of ECM1 (green) and PLSCR1 (green) throughout the epidermal layers (see asterisk). Scale bar, 50 μm.

does not occur intracellular and that PLSCR1 might be secreted by an unconventional secretory mechanism. The analysis of cultured HaCaT cells by immunogold electron microscopy revealed that ECM1 and PLSCR1 did not co-localize within the cytoplasm but co-localized outside the cell (Fig. 7D). Furthermore, both proteins occurred in the extracellular matrix produced by HaCaT cells (Fig. 7E).

Co-immunoprecipitation Studies on HaCaT Supernatant—In order to further confirm the secretion of PLSCR1 by keratinocytes and to establish the potency of secreted PLSCR1 to interact with ECM1a, co-immunoprecipitations were performed on supernatant of HaCaT cell cultures. Both immunoprecipitation with anti-PLSCR1 and detection with EDF anti-ECM1 as well as the reversed reaction show that a significant amount of protein interacts in the supernatant of these keratinocytes (Fig. 8A). These results demonstrate that secreted

PLSCR1 can effectively associate with ECM1a. Identical co-immunoprecipitation experiments were performed on 2-week-old air-exposed keratinocyte co-cultures with similar results (data not shown).

PLSCR1 Is Not Secreted through the Golgi Apparatus—Because PLSCR1 lacks a secretion signal peptide, we aimed to investigate whether or not the secretion of PLSCR1 continues through the classical Golgi-mediated secretory pathway. For this, the effect of brefeldin A on its secretion was investigated in HaCaT cell cultures (Fig. 8B). Cell surface transport of most plasma membrane proteins is sensitive to the drug brefeldin A. Brefeldin A blocks the recruitment of the small GTPase ARF1 (ADP-ribosylation factor 1) to the Golgi and the formation of COPI-coated vesicles. Inhibiting retrograde protein transport from the Golgi apparatus to the endoplasmic reticulum abolished the secretion of ECM1a, which does contain a hydrophobic secretion signal of 19 amino acids. However, the secretion of PLSCR1 by HaCaT cells was completely unaffected (Fig. 8B), demonstrating that PLSCR1 is secreted by an alternative, Golgi-independent pathway. The absence of PLSCR1 in the Golgi apparatus was further confirmed by co-localization studies using a Golgi-specific protein marker in HaCaT cells overexpressing eGFP-PLSCR1 (Fig. 9C) (see below).

Secretion of PLSCR1 Does Not Involve an Extracellular Membrane-bound Transition Phase—Because PLSCR1 is not secreted through the Golgi apparatus and a putative transmembrane helix is present, we next aimed to investigate whether its secretion might occur via a flip/flop mechanism. In the case of the latter, during the secretory process, a transient extracellular membrane-bound transition phase might be observed. For this, live HaCaT cells were stained for flow cytometric analysis with anti-PLSCR1 antibody for detection of membrane-bound PLSCR1 on the extracellular side of the cell membrane (Fig. 9A, MEMBRANE). However, no PLSCR1 expression could be detected on the extracellular side of the cell membrane. In contrast, following anti-PLSCR1 antibody staining and flow cytometric analysis of fixed and permeabilized HaCaT cells (Fig. 9A, INTRA-CELLULAR). PLSCR1 expression was readily detected. Therefore, we conclude that endogenous membrane-bound PLSCR1 is expressed on the intracellular side of the cell mem-

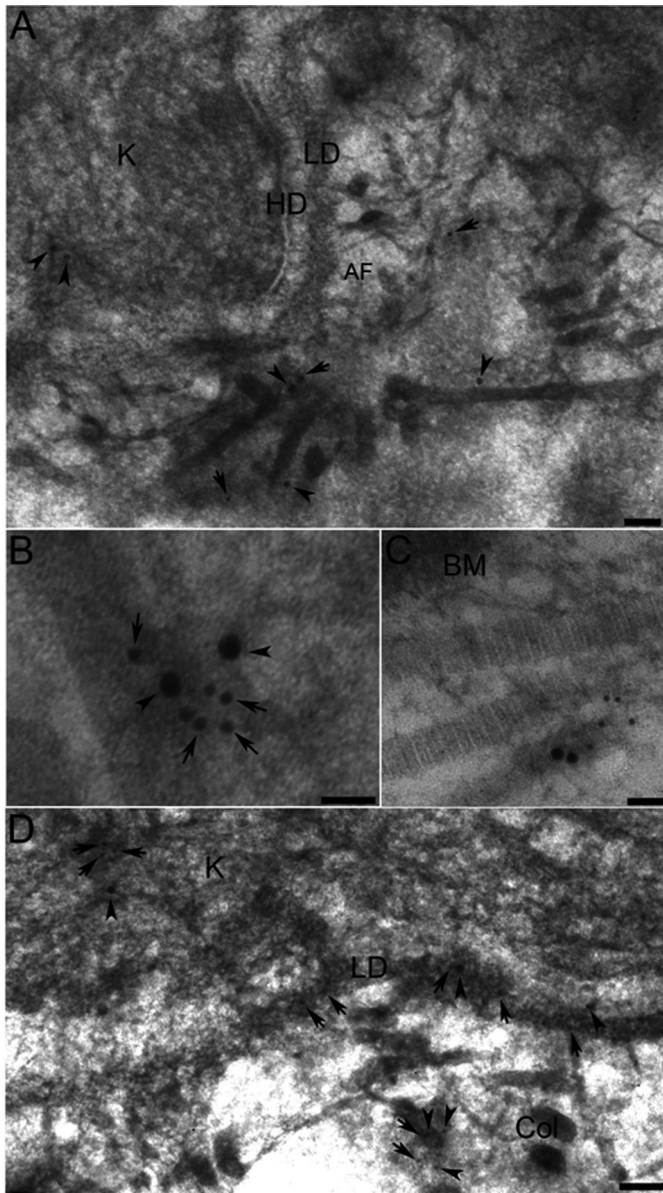


FIGURE 5. Ultrastructural localization of ECM1 and PLSCR1 on ultrathin sections of human skin. *A*, ECM1 (large gold particles, arrowheads) and PLSCR1 (small gold particles, arrows) are co-localized in the basal keratinocytes within the basement membrane zone and in close vicinity to dermal fibrils. *K*, keratinocyte; *HD*, hemidesmosome; *LD*, lamina densa; *AF*, anchoring fibrils. *B* and *C*, co-localization of ECM1 (large gold particles, arrowheads) and PLSCR1 (small gold particles, arrows) in network-like material in close vicinity to dermal collagen fibrils. *D*, ECM1 (large gold particles, arrowheads) and PLSCR1 (small gold particles, arrows) are both localized in the basal keratinocytes and are co-localized within the basement membrane zone (*LD*). *Col*, collagen fibrils. Scale bars, 100 nm (*A*, *C*, and *D*) and 50 μ m (*B*).

brane but not on the extracellular side of the cell membrane. Possibly, the detachment of PLSCR1 from the cell membrane is a relatively fast process and is difficult to detect using the above mentioned methodology. Therefore, we engineered HaCaT cells overexpressing an eGFP-PLSCR1 or HA-PLSCR1 fusion protein in order to detect low expression levels of PLSCR1 on the plasma membrane. The eGFP-PLSCR1-overexpressing cell line showed in the supernatants as well as in the cell lysate a higher concentration of PLSCR1 as compared with control HaCaT cells, both in the undifferenti-

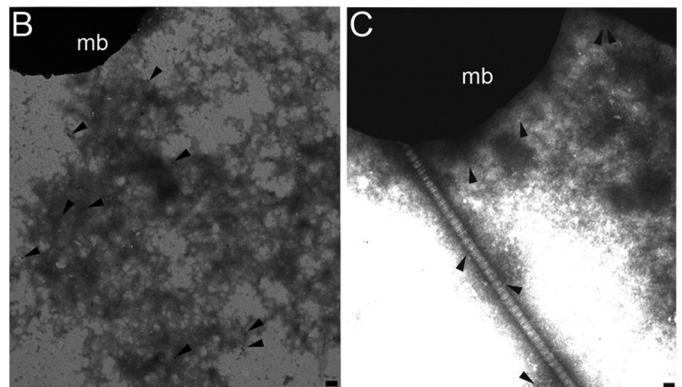
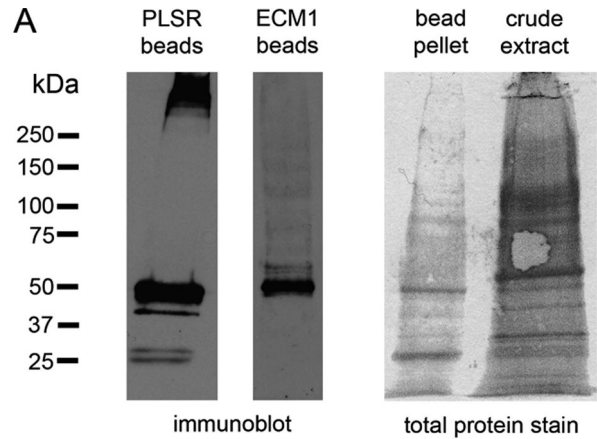


FIGURE 6. Isolation of ECM1- and PLSCR1-containing suprastructures from human skin by magnetic immunobeads. *A*, ECM1 was detected by immunoblotting in suprastructures by antibodies against PLSCR1 cross-linked to magnetic immunobeads (*lane 1*). By using magnetic immunobeads cross-linked to antibodies against ECM1, suprastructures containing PLSCR1 were isolated (*lane 2*). The blot membrane was stained with a total protein stain showing the ECM1 bead pellet (*lane 3*) and the crude extract of human skin (*lane 4*). *B* and *C*, extracellular matrix suprastructures isolated by magnetic immunobeads (*mb*) coated with either specific antibodies against ECM1 (*B*) or PLSCR1 (*C*). Immunogold electron microscopy revealed that the isolated suprastructures of the ECM1 bead pellet were labeled with antibodies against PLSCR1 (gold particles, arrowheads), and the isolated suprastructures of the PLSCR1 bead pellet were labeled with antibodies against ECM1 (gold particles, arrowheads). Scale bars, 200 nm.

ated state and following TPA stimulation (Fig. 9*B*). The HA-PLSCR1-overexpressing line only displayed increased expression of PLSCR1 in cell lysates of undifferentiated cells. However, following TPA stimulation, both in the supernatant and cell lysate, increased levels of PLSCR1 could be observed. Additionally, because overexpressed eGFP-PLSCR1 fusion protein may not reach the plasma membrane (*e.g.* because of incorrect folding), we investigated the cellular localization of eGFP-PLSCR1. Confocal microscopy results clearly demonstrate localization of eGFP-PLSCR1 fusion protein at the cell membrane, demonstrating normal processing of the overexpressed fusion protein (Fig. 9*C*). These data suggest successful overexpression of both constructs in HaCaT cells. However, following flow cytometric analysis, no membrane-bound PLSCR1 could be detected on the extracellular side of the cell membrane (Fig. 9*A*, *HACAT/eGFP-PLSCR1* row and *HACAT/HA-PLSCR1* row, *MEMBRANE* column), whereas clearly all overexpressed PLSCR1 was localized intracellularly (Fig. 9*A*, *HACAT/eGFP-PLSCR1* row and *HACAT/HA-PLSCR1* row,

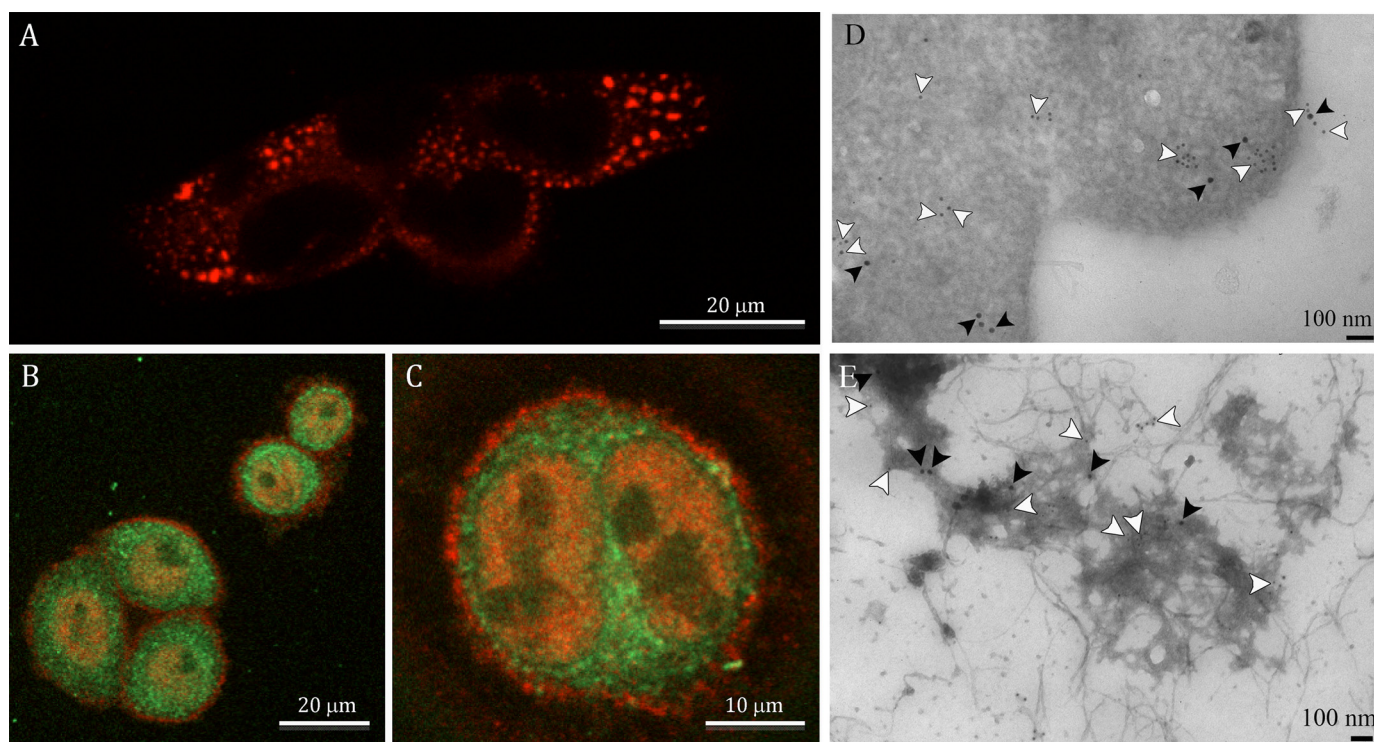


FIGURE 7. Confocal microscopic images of cultured HaCaT keratinocytes. *A*, ECM1 was stained with an anti-ECM1 antibody (EDF) and an anti-rabbit-Cy3 secondary antibody and is clearly visible in secretion vesicles. *B* and *C*, staining with the EDF rabbit anti-ECM1 and a secondary anti-rabbit-FITC (green) together with mouse anti-PLSCR1 C terminus and secondary anti-mouse-Cy3 (red). ECM1 can be found throughout the cytoplasm, whereas PLSCR1 is localized at the plasma membrane and the nucleus. There was no intracellular co-localization observed. *D*, ultrathin sections of cultured HaCaT keratinocytes showed no co-localization of ECM1 and PLSCR1 within the cytoplasm. Note that both proteins were co-localized out of the cell. Scale bar, 100 nm. *E*, extracellular matrix produced by HaCaT keratinocytes. ECM1 (black arrowheads) and PLSCR1 (white arrowheads) were co-localized in the matrix. Scale bar, 100 nm.

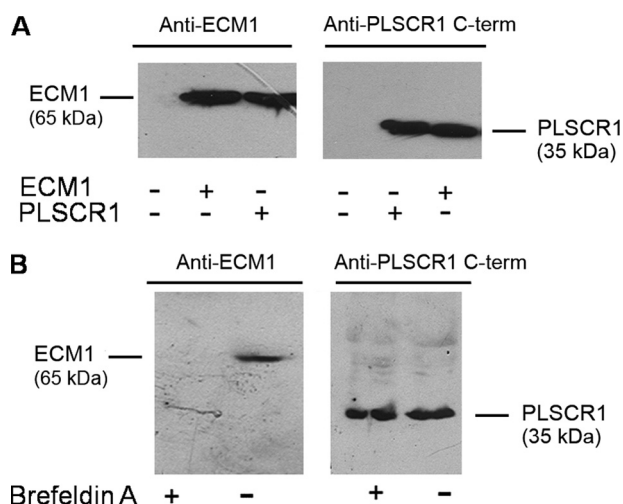


FIGURE 8. PLSCR1 is secreted by HaCaT cells in a brefeldin A-insensitive manner. *A*, supernatant from an overnight HaCaT culture was used for co-immunoprecipitation with anti-ECM1 (EDF) or polyclonal anti-PLSCR1 antibody, followed by immunoblotting with the complementary antibodies (EDF or PLSCR1 C terminus) as indicated (160 μ g of protein loaded). Non-immunoprecipitated supernatant and precipitation with the antibody used for visualization were used as controls (60 and 80 μ g of protein loaded, respectively). Both directions of co-immunoprecipitation are positive. *B*, HaCaT cells were incubated with brefeldin A at a nontoxic dose of 25 ng/ml for 48 h to inhibit Golgi-mediated secretion. Immunoblot with anti-ECM1 (EDF) or anti-PLSCR1 C terminus on the resulting supernatant reveals effective abolishment of the Golgi-mediated secretion of ECM1 when supernatant from brefeldin-treated cells is compared with supernatant from an untreated culture. The secretion of PLSCR1 was not sensitive to brefeldin A.

INTRA-CELLULAR column). Based on the above described data, we conclude that the secretion or translocation of PLSCR1 does not involve a transient extracellular membrane-bound transition phase. In order to further clarify the membrane localization of PLSCR1, we next investigated whether palmitoylation is necessary for the secretion of PLSCR1. Therefore, HaCaT cells were cultured under the condition where palmitoylation was metabolically prevented by 2-bromo-palmitate, a competitive inhibitor of the transfer of palmitoyl-CoA to the cysteinoyl thiol (25). However, no altered secretion of PLSCR1 was observed when comparing the supernatant and cell lysate of HaCaT cells stably overexpressing eGFP-PLSCR1 in the presence or absence of 2-bromo-palmitate (2-BP) (Fig. 9D). In addition, although a small amount of eGFP-PLSCR1 was translocated to the nucleus following inhibition of palmitoylation in HaCaT/eGFP-PLSCR1 cells (Fig. 9E, +2-BP), the majority of eGFP-PLSCR1 was still localized at the cell membrane (Fig. 9E, +2-BP) as compared with untreated HaCaT/eGFP-PLSCR1 cells (Fig. 9E, control). These data suggest that palmitoylation is most likely not involved in the trafficking and secretion of PLSCR1.

PLSCR1 Secretion via a Lipid Raft-dependent Pathway—In a final step to elucidate a potential mechanism for secretion of PLSCR1 in the extracellular matrix, we investigated the involvement of trafficking via lysosomal and/or endosomal vesicles. Confocal microscopy results clearly exclude the involvement of lysosomal vesicles because no co-localization of eGFP-PLSCR1 was observed with LAMP-1 (lysosome-associated

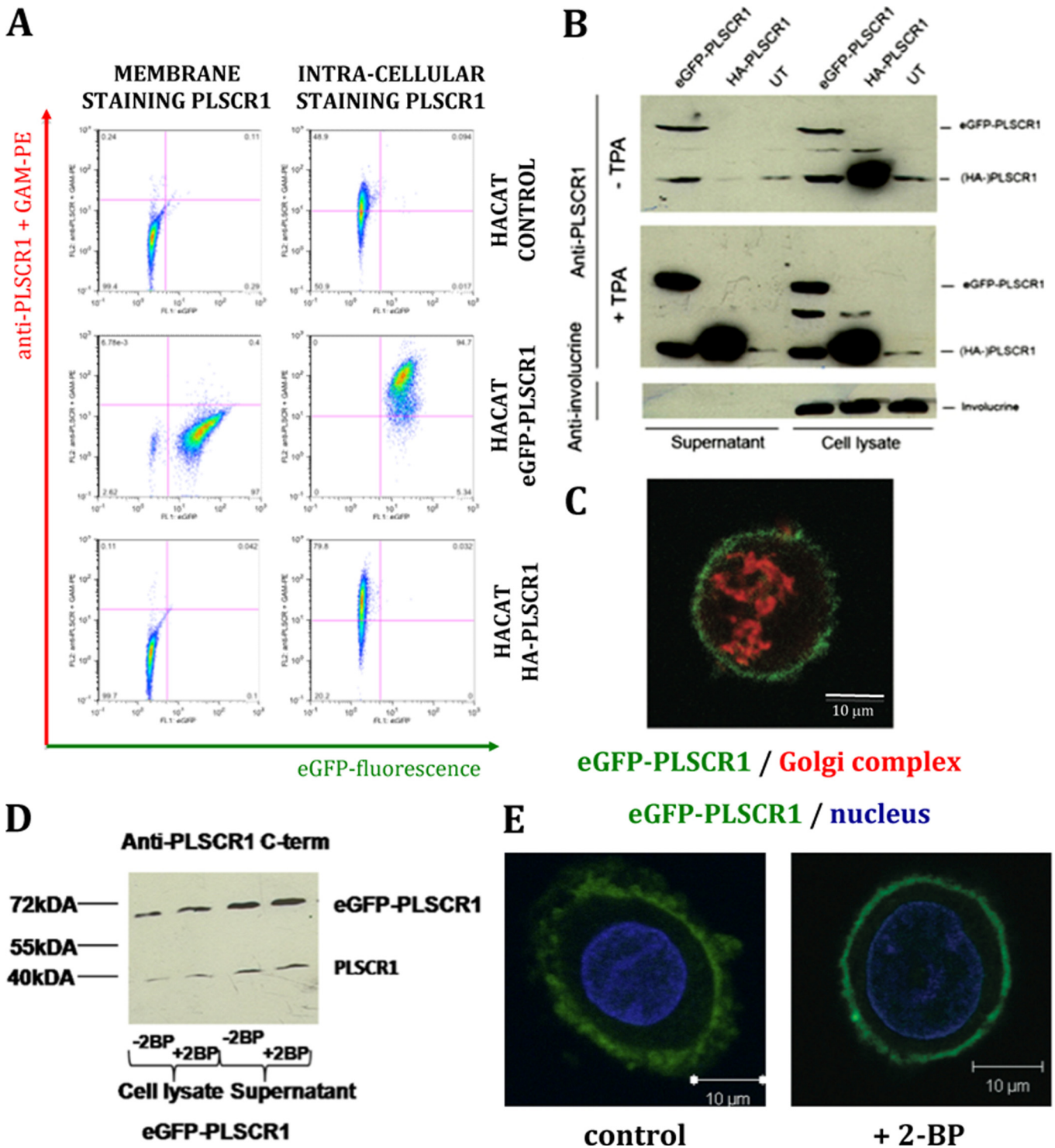


FIGURE 9. Intracellular localization of endogenous PLSCR1 and overexpressed PLSCR1. *A*, HaCaT, HaCaT/eGFP-PLSCR1, and HaCaT/HA-PLSCR1 cell lines were analyzed by flow cytometry for the expression of extracellular membrane-bound (*MEMBRANE*) or intracellular (*INTRA-CELLULAR*) PLSCR1 localization. *x* axis, eGFP fluorescence indicating overexpression of eGFP-PLSCR fusion protein in HaCaT/eGFP-PLSCR1 cells. *y* axis, anti-PLSCR + GAM-PE fluorescence indicating intracellular overexpression of PLSCR1 in HaCaT/eGFP-PLSCR1 and HaCaT/HA-PLSCR1 cells, as compared with HaCaT control cells. *B*, HaCaT, HaCaT/eGFP-PLSCR1, and HaCaT/HA-PLSCR1 cell lines were analyzed by immunoblot for expression of endogenous PLSCR1 protein or HA-PLSCR1 fusion protein (HA-PLSCR1) and eGFP-PLSCR1 fusion protein (eGFP-PLSCR1), both in the supernatant and in cell lysates. Results indicate PLSCR1 overexpression in the supernatant and cell lysate of HaCaT/eGFP-PLSCR1 cells and in the cell lysate of HaCaT/HA-PLSCR1 cells, as compared with detection in both supernatant and cell lysate of control HaCaT cells. Upon TPA stimulation, high levels of PLSCR1 are detected both in the supernatant and cell lysate of all cell lines. *C*, HaCaT/eGFP-PLSCR1 cells were immunostained with the 58-kDa Golgi complex-specific marker (*red fluorescence*) and analyzed by confocal microscopy to determine membrane localization of the eGFP-PLSCR fusion protein (*green fluorescence*). *D*, HaCaT/eGFP-PLSCR1 cells treated with the palmitoylation inhibitor 2-bromo-palmitate (*2-BP*) were analyzed by immunoblot for expression of endogenous PLSCR1 protein or eGFP-PLSCR1 fusion protein, both in the supernatant and in cell lysate. Results indicate no difference as compared with control HaCaT cells (see Fig. 10*B*). *E*, HaCaT/eGFP-PLSCR1 cells (control) and HaCaT/eGFP-PLSCR1 cells treated with 2-bromo-palmitate (+2-BP) were stained with DAPI (blue fluorescence indicating the nucleus) and analyzed by confocal microscopy to determine localization of the eGFP-PLSCR fusion protein (*green fluorescence*).

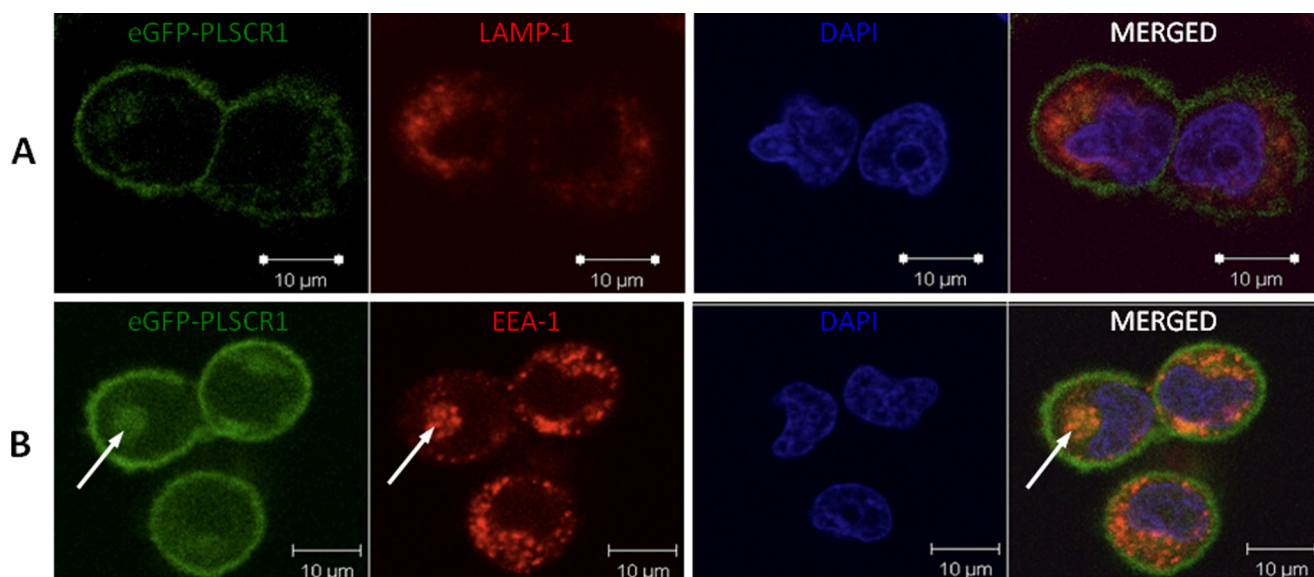


FIGURE 10. **Partial co-localization of PLSCR1 in endosomes but not in lysosomes.** HACAT/eGFP-PLSCR1 cells were immunostained with LAMP-1-specific marker (red fluorescence) and DAPI (nucleus, blue fluorescence) (A) or the EEA-1-specific marker (red fluorescence) and DAPI (nucleus, blue fluorescence) (B) and analyzed by confocal microscopy to determine localization of the eGFP-PLSCR fusion protein (green fluorescence). White arrows, partial co-localization of eGFP-PLSCR1 fusion protein with EEA-1-stained endosomes.

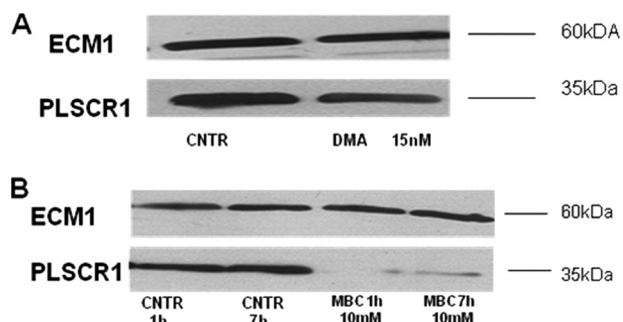


FIGURE 11. **Effect of dimethyl- β -cyclodextrin (MBC) and dimethyl amiloride (DMA) treatment on HaCaT cells.** Representative Western blot showing inhibition of PLSCR1 release from methyl- β -cyclodextrin-treated HaCaT cells with 10 mM MBC for 1 or 7 h at 37 °C. There was no effect of 15 nM dimethyl amiloride treatment for 7 h at 37 °C on PLSCR1 secretion in HaCaT cells. CNTR, control.

membrane protein 1)-stained lysosomes (Fig. 10A). In contrast, partial co-localization of eGFP-PLSCR1 was observed with EEA-1 (early endosome antigen 1)-stained endosomes (Fig. 10B). This suggests the export of PLSCR1 via intracellular vesicles, most likely endosomes or exosomes, which are formed through the inward budding of late endosomal membranes. As shown in Fig. 11A, pretreatment of HaCaT cells with 15 nM dimethyl amiloride, an exosome inhibitor, had no significant effect on PLSCR1 release from these cells. In contrast, treatment with methyl- β -cyclodextrin (10 nM), an inhibitor of lipid formation via depletion of membrane cholesterol, had no effect on ECM1 release but completely reduced the release of PLSCR1 (Fig. 11B). Therefore, whereas part of the produced PLSCR1 has an intracellular membrane function, another part is alternatively secreted via a lipid raft-dependent pathway in order to interact with ECM1a in the extracellular matrix.

DISCUSSION

The mechanisms by which the *ECM1*-encoded proteins exert their biological function(s) are still not resolved, although

there are indications for their involvement in biological processes like cell proliferation, angiogenesis, chondrogenesis, skin biology, and cancer (for a review, see Refs. 33 and 34).

In order to gain some insight into the biological function of the ECM1a protein, we performed a yeast two-hybrid screening with full-length ECM1a and a shorter fragment (SASDL2+, aa 177–361). Computational homology modeling identified within ECM1a four domains: an NH₂-terminal domain forming α -helices (α D1), followed by three SASDL domains, 2–4, topologically comparable with the subdomain of the third serum albumin domain (9). SASDL2+, which contains a piece of exon 6 and the complete alternatively spliced exon 7, includes a part of the two tandem repeat domains of ECM1a (aa 151–405) (Fig. 3A) (1, 8). Approximately 50% of the mutations in patients with lipid proteinosis cluster to exons 6 and 7 of the *ECM1* gene, which makes this an attractive region to look for protein interaction partners of ECM1a (35).

Previous studies have reported interactions of ECM1 with proteins like perlecan (6), fibulin 1C/D (19), fibulin-3 (9), matrix metalloproteinase 9 (20), fibronectin (20, 36), collagen type IV, and laminin 332 (36). In the present study, we report that ECM1a interacts with phospholipid scramblase 1, PLSCR1. Biochemical approaches revealed that PLSCR1 interacts with the carboxyl part of tandem repeat one and the N-terminal part of tandem repeat 2 (aa 203–349) encoding mainly exon 7 and present only in ECM1a. This implies that PLSCR1 is a specific protein interaction partner of ECM1a/c because exon 7 is deleted by alternative splicing from ECM1b. We cannot discriminate between the isoforms ECM1a and ECM1c, which differ by 19 aa in a cysteine-free domain encoded by exon 5a. ECM1a expression is almost completely restricted to the basal cell layer and the basal lamina, whereas ECM1b is located in the suprabasal epidermal layers of human skin (3, 5). Thus, the binding of PLSCR1 to ECM1a must be restricted to the basal cell layer and/or the DEJ zone of human skin. This is in agree-

ment with the observation that ECM1a and PLSCR1 co-localize at the basal layer on human skin sections and at the DEJ zone of *in vitro* reconstructed human skin (see Fig. 4).

In 2002, loss-of-function mutations in the *ECM1* gene were identified in subjects with the autosomal recessive skin disorder lipoid proteinosis (15). Lipoid proteinosis is mainly a mucocutaneous disorder characterized by laryngeal infiltration leading to hoarseness and generalized thickening and scarring of the skin and mucosae. In lipoid proteinosis patients, areas of the skin habitually exposed to the sun may show a more severely scarred and photoaged appearance when compared with the rest of the body (37). Interestingly, ECM1 was found to be up-regulated by UV in human skin (5). UV light is a well established DNA mutagen and triggers the p53-mediated intrinsic mode of apoptosis in keratinocytes (38). UV irradiation of intact cells overexpressing PLSCR1 stimulates the production of phosphatidylserine and directs it to the surface regions of the membrane (39). PKC- δ is able to activate PLSCR1, which is believed to be a major regulator of phosphatidylserine externalization during apoptosis (39), directly by phosphorylating its threonine 161 and indirectly by increasing the Ca²⁺ and phorbol ester concentration. However, the role of PKC- δ in increasing PLSCR1 activity during apoptosis is not well established. Increased PLSCR1 activity amplified UV-mediated apoptosis primarily through the activation of the intrinsic apoptotic pathway (caspase 3 and 9) (39). Thus, it is possible that irradiation of skin with UV will activate the PKC- δ pathway, which could lead, through activation of PLSCR1, to up-regulation of the ECM1 protein.

The expression of the *ECM1* gene in keratinocytes can be modulated *in vitro* by diffusible growth factor(s) secreted by stromal cells (3). In this study, we used human skin equivalents to identify whether growth factors are able to stimulate the expression of ECM1 and/or PLSCR1. We tested EGF as a growth factor because this protein is known to induce basement membrane formation in organotypic keratinocyte monocultures (32). EGF is also able to activate PLSCR1 by inducing PLSCR1 to bind to the EGF receptor (EGFR) (40, 41). Furthermore, human skin equivalents have been used because of the crucial role fibroblasts play in basement membrane formation (27, 32). Factors released by fibroblasts resulted in the expression of basement membrane components (*e.g.* collagen type IV and VII, laminin 332, nidogen, BP-180, and LAD-1) in organotypic keratinocyte monocultures (32). In this study, similar results have been obtained for the ECM1 molecule as well as for PLSCR1, demonstrating that ECM1 and PLSCR1 were deposited and localize at the DEJ zone in reconstructed skin. This is in agreement with our observations identifying ECM1 as a basement membrane component of the human skin (36). In non-stimulated organotypic keratinocyte monocultures, ECM1 and PLSCR1 were not expressed, whereas cultures treated with EGF revealed an up-regulation of both proteins. This finding indicates that dermal/epidermal interaction through fibroblasts seems to be essential for the synthesis of both molecules. This interaction can be based upon 1) production of soluble factors by either epithelial (after being activated by, for example, growth factors) or mesenchymal cells that exhibit autocrine and/or paracrine activities, 2) cell-matrix interactions, or 3) sig-

naling by direct cell-cell contact. Through the release of interleukin-1, keratinocytes can enhance the release of growth factors such as granulocyte-macrophage colony-stimulating factor, IL-6, or IL-8 in dermal cells, which in turn stimulate basement membrane formation (42–45). Thus, we have demonstrated that, in the absence of fibroblasts, EGF can be used as a substitute to provide keratinocyte growth and differentiation and can also stimulate ECM1 as well as PLSCR1 expression. The mechanism of how, PLSCR1 and ECM1 affect cell proliferation and differentiation in response to selective growth factors (*e.g.* EGF) remains to be determined.

Due to the topological separation of the secreted ECM1 and membrane-bound, endofacial PLSCR1, we looked for the place of interaction. Electron micrographs of human skin reveal that PLSCR1 is secreted into the extracellular matrix and co-localizes with ECM1 around the basal membrane in the DEJ zone and within network-like suprastructures in close vicinity to dermal fibrils (Figs. 5 and 6). In HaCaT cultures, we detected secretion of PLSCR1 and effective interaction with ECM1 in the supernatant as well as the co-localization of both proteins in the extracellular matrix of these cells (Figs. 7, *D* and *E*, and 8*A*). Together, these results suggest physiologically relevant secretion of PLSCR1 by keratinocytes, although we did not yet investigate secretion of PLSCR1 by other cell types.

Most secreted proteins contain a secretion signal, and transport to the extracellular space is mediated by an endoplasmic reticulum/Golgi-dependent secretory pathway. The fact that PLSCR1 does not contain a signal peptide suggested that it might be secreted by an alternative secretory mechanism, collectively termed unconventional secretory process (46). The extracellular appearance of PLSCR1 is not compromised in the presence of brefeldin A, an inhibitor of retrograde protein transport through the Golgi apparatus, whereas ECM1 secretion was completely abolished. PLSCR1 secretion thus appears to be mediated by a Golgi-independent secretory pathway and is thus a novel member of a growing class of extracellular proteins exported by an unconventional secretory route. There are several alternative pathways that could mediate PLSCR1 secretion and have recently been reviewed (46). These include 1) export via intracellular vesicles, most likely endosomes; 2) exosomes; 3) direct transport across the membrane; and 4) a flip-flop mechanism.

The finding that PLSCR1 is secreted by an unconventional secretory process was unexpected and is of great importance in the understanding of the three-dimensional structure of PLSCR1. Recently, a three-dimensional model for PLSCR1 has been proposed, predicting that this protein is attached to the membrane only through palmitoylation, without the involvement of a transmembrane domain (47). We could not observe any PLSCR1 protein present on the membrane of HaCaT cells in FACS experiments, when stained with a polyclonal antibody against PLSCR1 or an antibody directed against the C terminus of PLSCR1 (aa 306–318, which up to now was considered as the extracellular domain of PLSCR1) (23). Our studies do not support the above mentioned computational model in that we were able to show non-involvement of the palmitoylation in the membrane translocation (Fig. 9), thereby excluding the membrane translocation option and an energetically very unlikely

flip-flop mechanism. Confocal imaging experiments also excluded the possibility of PLSCR1 secretion by lysosomal transport. However, partial localization of PLSCR1 in endosomal vesicles suggested the participation of endosomes and/or exosomes in the endocytic trafficking and secretion of PLSCR1 (Fig. 10). This observation is not unexpected because PLSCR3 has already been reported to reside in exosomes from a human tumor cell line (48). However, treatment of HaCaT cell cultures with dimethyl amiloride, an exosome inhibitor, had no significant effect on PLSCR1 release. In contrast, treatment of HaCaT cultures with methyl- β -cyclodextrin, a lipid raft-disrupting drug, completely blocked the secretion of PLSCR1 (Fig. 11). Thus, these findings are in keeping with the participation of lipid rafts in forming surface delivery and exit sites for PLSCR1 secretion. TNF α , delivered to phagocytic cups, is an example of cytokine secretion via a cholesterol-rich lipid raft-dependent manner (49). Further investigations will be necessary to unravel the mechanism by which lipid rafts become the site of delivery for PLSCR1. PLSCR1 in lipid rafts also interacts with EGFR. Stimulation by EGF of cells expressing EGFR leads to a physical association of PLSCR1 with the activated EGFR and the adaptor protein Shc, resulting in tyrosine phosphorylation of PLSCR1 (50). In this context, it is important to note that both proteins, PLSCR1 and ECM1, are expressed at the DEJ zone in reconstructed skin equivalents after stimulation with EGF. Taken together, our results identify PLSCR1 as well as ECM1 as being involved in EGF-dependent signal transduction and provide the framework to study the cellular function of PLSCR1 outside the cell.

In summary, although PLSCR1 is a member of the PLSCR gene family of type II transmembrane endofacial plasma membrane proteins and is thought to contribute to the translayer movement of phosphatidylserine (“scrambling”) and other membrane phospholipids, the function of PLSCR1 as a scramblase has been challenged (23, 41, 46, 51–53). From recent studies, it is becoming clear that the proteins labeled as “phospholipid scramblases” are not required for scramblase activation or activity (for an update on PLSCR, consult Ref. 54). Involvement of PLSCR1 in protein-protein interaction is becoming more evident. It has been proposed that PLSCR1 interacts with several cellular proteins involved in signaling pathways and acts as a transcription factor for the inositol 1,4,5-triphosphate receptor type 1 gene (23, 53). In this study, we identified ECM1a as a novel protein interaction partner of PLSCR1 in human skin. More research will be needed to clarify the physiological significance of this interaction. Recently, PLSCR1 was also identified as a cellular receptor for the secretory leukocyte protease inhibitor. It has been shown that the interaction between CD4 and PLSCR1 is disrupted upon secretory leukocyte protease inhibitor binding (28).

In our study, we demonstrate for the first time that PLSCR1, in addition to its intracellular role, can also function outside the cell. We demonstrate that, in addition to membrane localization and function, part of translated PLSCR1 protein is secreted and interacts with the tandem repeat region of ECM1a in the DEJ zone of human skin. Therefore, PLSCR1 belongs to a growing family of single proteins with functions, both inside and

outside the cell (for a review, see Ref. 55), whereby PLSCR1, together with ECM1, may play a regulatory role in human skin.

Acknowledgment—We thank the Service Facility of the Laboratory of Cell Biology of the University of Antwerp for assistance with the confocal electron microscopy experiments.

REFERENCES

- Smits, P., Ni, J., Feng, P., Wauters, J., Van Hul, W., Boutaibi, M. E., Dillon, P. J., and Merregaert, J. (1997) *Genomics* **45**, 487–495
- Johnson, M. R., Wilkin, D. J., Vos, H. L., Ortiz de Luna, R. I., Dehejia, A. M., Polymeropoulos, M. H., and Francomano, C. A. (1997) *Matrix Biol.* **16**, 289–292
- Smits, P., Poumay, Y., Karperien, M., Tylzanowski, P., Wauters, J., Huylebroeck, D., Ponc, M., and Merregaert, J. (2000) *J. Invest. Dermatol.* **114**, 718–724
- Oyama, N., Chan, I., Neill, S. M., South, A. P., Wojnarowska, F., Kawakami, Y., D’Cruz, D., Mepani, K., Hughes, G. J., Bhogal, B. S., Kaneko, F., Black, M. M., and McGrath, J. A. (2004) *J. Clin. Invest.* **113**, 1550–1559
- Sander, C. S., Sercu, S., Ziemer, M., Hipler, U. C., Elsner, P., Thiele, J. J., and Merregaert, J. (2006) *Br. J. Dermatol.* **154**, 218–224
- Mongiati, M., Fu, J., Oldershaw, R., Greenhalgh, R., Gown, A. M., and Iozzo, R. V. (2003) *J. Biol. Chem.* **278**, 17491–17499
- Horev, L., Potikha, T., Ayalon, S., Molho-Pessach, V., Ingber, A., Gany, M. A., Edin, B. S., Glaser, B., and Zlotogorski, A. (2005) *Exp. Dermatol.* **14**, 891–897
- Bhalerao, J., Tylzanowski, P., Filie, J. D., Kozak, C. A., and Merregaert, J. (1995) *J. Biol. Chem.* **270**, 16385–16394
- Sercu, S., Lambeir, A. M., Steenackers, E., El Ghalbzouri, A., Geentjens, K., Sasaki, T., Oyama, N., and Merregaert, J. (2009) *Matrix Biol.* **28**, 160–169
- Deckers, M. M., Smits, P., Karperien, M., Ni, J., Tylzanowski, P., Feng, P., Parmelee, D., Zhang, J., Bouffard, E., Gentz, R., Löwik, C. W., and Merregaert, J. (2001) *Bone* **28**, 14–20
- Kong, L., Tian, Q., Guo, F., Mucignat, M. T., Perris, R., Sercu, S., Merregaert, J., Di Cesare, P. E., and Liu, C. J. (2010) *Matrix Biol.* **29**, 276–286
- Han, Z., Ni, J., Smits, P., Underhill, C. B., Xie, B., Chen, Y., Liu, N., Tylzanowski, P., Parmelee, D., Feng, P., Ding, I., Gao, F., Gentz, R., Huylebroeck, D., Merregaert, J., and Zhang, L. (2001) *FASEB J.* **15**, 988–994
- Anderson, C. A., Massey, D. C., Barrett, J. C., Prescott, N. J., Tremelling, M., Fisher, S. A., Gwilliam, R., Jacob, J., Nimmo, E. R., Drummond, H., Lees, C. W., Onnie, C. M., Hanson, C., Blaszczyk, K., Ravindrarajah, R., Hunt, S., Varma, D., Hammond, N., Lewis, G., Attlesey, H., Watkins, N., Ouwehand, W., Strachan, D., McArdle, W., Lewis, C. M., Lobo, A., Sanderson, J., Jewell, D. P., Deloukas, P., Mansfield, J. C., Mathew, C. G., Satsangi, J., and Parkes, M. (2009) *Gastroenterology* **136**, 523–529
- Urbach, E., and Wietke, C. (1929) *Virchows Arch. Path. Anat.* **273**, 285–319
- Hamada, T., McLean, W. H., Ramsay, M., Ashton, G. H., Nanda, A., Jenkins, T., Edelstein, I., South, A. P., Bleck, O., Wessagowit, V., Mallipeddi, R., Orchard, G. E., Wan, H., Dopping-Hepenstal, P. J., Mellerio, J. E., Whittock, N. V., Munro, C. S., van Steensel, M. A., Steijlen, P. M., Ni, J., Zhang, L., Hashimoto, T., Eady, R. A., and McGrath, J. A. (2002) *Hum. Mol. Genet.* **11**, 833–840
- Hamada, T., Wessagowit, V., South, A. P., Ashton, G. H., Chan, I., Oyama, N., Siriwhattana, A., Jewhasuchin, P., Charuwichitratana, S., Thappa, D. M., Jeevankumar, B., Lenane, P., Krafchik, B., Kulthanan, K., Shimizu, H., Kaya, T. I., Erdal, M. E., Paradisi, M., Paller, A. S., Seishima, M., Hashimoto, T., and McGrath, J. A. (2003) *J. Invest. Dermatol.* **120**, 345–350
- Oyama, N., Chan, I., Neill, S. M., Hamada, T., South, A. P., Wessagowit, V., Wojnarowska, F., D’Cruz, D., Hughes, G. J., Black, M. M., and McGrath, J. A. (2003) *Lancet* **362**, 118–123
- Chan, I., Oyama, N., Neill, S. M., Wojnarowska, F., Black, M. M., and McGrath, J. A. (2004) *Clin. Exp. Dermatol.* **29**, 499–504
- Fujimoto, N., Terlizzi, J., Brittingham, R., Fertala, A., McGrath, J. A., and Uitto, J. (2005) *Biochem. Biophys. Res. Commun.* **333**, 1327–1333
- Fujimoto, N., Terlizzi, J., Aho, S., Brittingham, R., Fertala, A., Oyama, N.,

- McGrath, J. A., and Uitto, J. (2006) *Exp. Dermatol.* **15**, 300–307
21. Fields, S., and Song, O. (1989) *Nature* **340**, 245–246
 22. Huang, Y., Zhao, Q., and Chen, G. Q. (2006) *Acta. Physiol. Sinica* **58**, 501–510
 23. Sahu, S. K., Gummadi, S. N., Manoj, N., Aradhyam, G. K. (2007) *Arch. Biochem. Biophys.* **462**, 103–114
 24. Ponec, M., Weerheim, A., Kempenaar, J., Mulder, A., Gooris, G. S., Bouwstra, J., and Mommaas, A. M. (1997) *J. Invest. Dermatol.* **109**, 348–355
 25. Laniosz, V., Dabydeen, S. A., Havens, M. A., and Meneses, P. I. (2009) *J. Virol.* **83**, 8221–8232
 26. Webb, Y., Hermida-Matsumoto, L., and Resh, M. D. (2000) *J. Biol. Chem.* **275**, 261–270
 27. el-Ghalbzouri, A., Gibbs, S., Lamme, E., Van Blitterswijk, C. A., and Ponec, M. (2002) *Br. J. Dermatol.* **147**, 230–243
 28. Py, B., Basmaciogullari, S., Bouchet, J., Zarka, M., Moura, I. C., Benhamou, M., Monteiro, R. C., Hocini, H., Madrid, R., and Benichou, S. (2009) *PLoS ONE* **4**, e5006
 29. Ponsaerts, P., Brown, J. P., Van den Plas, D., Van den Eeden, L., Van Bockstaele, D. R., Jorens, P. G., Van Tendeloo, V. F., Merregaert, J., Singh, P. B., and Berneman, Z. N. (2004) *Gene Ther.* **11**, 1606–1610
 30. Kassner, A., Hansen, U., Miosge, N., Reinhardt, D. P., Aigner, T., Bruckner-Tuderman, L., Bruckner, P., and Grässel, S. (2003) *Matrix Biol.* **22**, 131–143
 31. Villone, D., Fritsch, A., Koch, M., Bruckner-Tuderman, L., Hansen, U., and Bruckner, P. (2008) *J. Biol. Chem.* **283**, 24506–24513
 32. El Ghalbzouri, A., Jonkman, M. F., Dijkman, R., and Ponec, M. (2005) *J. Invest. Dermatol.* **124**, 79–86
 33. Sercu, S., Oyama, N., and Merregaert, J. (2010) *Textbook of Aging Skin* (Farage, M. A., Miller, K. W., and Maibach, H. I., eds) pp. 77–91, Springer-Verlag, Berlin
 34. Sercu, S., Zhang, L., and Merregaert, J. (2008) *Cancer Invest.* **26**, 375–384
 35. Chan, I., Liu, L., Hamada, T., Sethuraman, G., and McGrath, J. A. (2007) *Exp. Dermatol.* **16**, 881–890
 36. Sercu, S., Zhang, M., Oyama, N., Hansen, U., El Ghalbzouri, A., Jun, G., Geentjens, K., Zhang, L., and Merregaert, J. (2008) *J. Invest. Dermatol.* **128**, 1397–1408; Correction *J. Invest. Dermatol.* (2009) **129**, 1836–1837
 37. Van Hougenhouck-Tulleken, W., Chan, I., Hamada, T., Thornton, H., Jenkins, T., McLean, W. H., McGrath, J. A., and Ramsay, M. (2004) *Br. J. Dermatol.* **151**, 413–423
 38. Kulms, D., Pöppelmann, B., Yarosh, D., Luger, T. A., Krutmann, J., and Schwarz, T. (1999) *Proc. Natl. Acad. Sci. U.S.A.* **96**, 7974–7979
 39. Yu, A., McMaster, C. R., Byers, D. M., Ridgway, N. D., and Cook, H. W. (2004) *Biochem J.* **381**, 609–618
 40. Sun, J., Nanjundan, M., Pike, L. J., Wiedmer, T., and Sims, P. J. (2002) *Biochemistry* **41**, 6338–6345
 41. Nanjundan, M., Sun, J., Zhao, J., Zhou, Q., Sims, P. J., and Wiedmer, T. (2003) *J. Biol. Chem.* **278**, 37413–37418
 42. Smola, H., Thiekötter, G., and Fusenig, N. E. (1993) *J. Cell. Biol.* **122**, 417–429
 43. Waelti, E. R., Inaebnit, S. P., Rast, H. P., Hunziker, T., Limat, A., Braathen, L. R., and Wiesmann, U. (1992) *J. Invest. Dermatol.* **98**, 805–808
 44. Boxman, I. L., Ruwhof, C., Boerman, O. C., Löwik, C. W., and Ponec, M. (1996) *Arch. Dermatol. Res.* **288**, 391–398
 45. Werner, S., and Smola, H. (2001) *Trends Cell. Biol.* **11**, 143–146
 46. Nickel, W., and Rabouille, C. (2009) *Nat. Rev. Mol. Cell. Biol.* **10**, 148–155
 47. Bateman, A., Finn, R. D., Sims, P. J., Wiedmer, T., Biegert, A., and Söding, J. (2009) *Bioinformatics* **25**, 159–162
 48. Mathivanan, S., Lim, J. W., Tauro, B. J., Ji, H., Moritz, R. L., and Simpson, R. J. (2010) *Mol. Cell. Proteomics* **9**, 197–208
 49. Kay, J. G., Murray, R. Z., Pagan, J. K., and Stow, J. L. (2006) *J. Biol. Chem.* **281**, 11949–11954
 50. Wiedmer, T., Zhao, J., Nanjundan, M., and Sims, P. J. (2003) *Biochemistry* **42**, 1227–1233
 51. Dong, B., Zhou, Q., Zhao, J., Zhou, A., Harty, R. N., Bose, S., Banerjee, A., Slee, R., Guenther, J., Williams, B. R., Wiedmer, T., Sims, P. J., and Silverman, R. H. (2004) *J. Virol.* **78**, 8983–8993
 52. Nakamaki, T., Okabe-Kado, J., Yamamoto-Yamaguchi, Y., Hino, K., Tomoyasu, S., Honma, Y., and Kasukabe, T. (2002) *Exp. Hematol.* **30**, 421–429
 53. Zhou, Q., Ben-Efraim, I., Bigcas, J. L., Junqueira, D., Wiedmer, T., and Sims, P. J. (2005) *J. Biol. Chem.* **280**, 35062–35068
 54. Bevers, E. M., and Williamson, P. L. (2010) *FEBS Lett.* **584**, 2724–2730
 55. Radisky, D. C., Stallings-Mann, M., Hirai, Y., and Bissell, M. J. (2009) *Nat. Rev. Mol. Cell. Biol.* **10**, 228–234